Phylogenetic and Environmental Context of a Tournaisian Tetrapod Fauna

Jennifer A. Clack[1], Carys E. Bennett[3], David K. Carpenter[4], Sarah J. Davies[3], Nicholas C. Fraser[5], Timothy I. Kearsey[6], John E. A. Marshall[4], David Millward[6], Benjamin K. A. Otoo[1,2], Emma J. Reeves [4], Andrew J. Ross[5], Marcello Ruta[7], Keturah Z. Smithson[1], Timothy R. Smithson[1] & Stig A. Walsh[5].

Author Affiliations

[1]J. A. Clack, K. Z. Smithson, T. R. Smithson, [1,2]B. K. A. Otoo† University Museum of Zoology Cambridge, Downing St., Cambridge CB2 3EJ, UK

[3]C. E. Bennett, S. J. Davies, Department of Geology, University of Leicester, Leicester, LE1 7RH, UK

[4]D. K. Carpenter, J. E. A. Marshall, E. J. Reeves, National Oceanography Centre University of Southampton, Waterfront Campus European Way, Southampton, SO14 3ZH UK

[5]N. C Fraser, S. Walsh, A. J. Ross, National Museum of Scotland, Chambers St., Edinburgh, EH1 1JF, UK

[6]T I. Kearsey, D. Millward, British Geological Survey, The Lyell Centre, Research Avenue South, Edinburgh, EH14 4AP, UK

[7] M. Ruta, School of Life Sciences, University of Lincoln, Joseph Banks Laboratories, Green Lane, Lincoln LN6 7DL, UK

†current address, [2]School of Earth Sciences, University of Bristol, Bristol, BS8 1RJ, UK

Summary

The end-Devonian to mid-Mississippian time interval has long been known for its depauperate palaeontological record, especially for tetrapods. This interval encapsulates the time of increasing terrestriality among tetrapods, but only two Tournaisian localities previously produced tetrapod fossils. Here we describe five new Tournaisian tetrapods (*Perittodus apsconditus*, *Koilops herma*, *Ossirarus kierani*, *Diploradus austiumensis* and *Aytonerpeton microps*) from two localities in their environmental context. A phylogenetic analysis retrieved three taxa as stem tetrapods, interspersed among Devonian and Carboniferous forms, and two as stem amphibians, suggesting a deep split among crown tetrapods. We also illustrate new tetrapod specimens from these and additional localities in the Borders Region of Scotland. The new taxa and specimens suggest that tetrapod diversification was well established by the Tournaisian. Sedimentary evidence indicates that tetrapod fossils are usually associated with sandy siltstones overlying wetland palaeosols. Tetrapods were probably living on vegetated surfaces subsequently flooded. We show that atmospheric oxygen levels were stable across the Devonian/Carboniferous boundary, and did not inhibit the evolution of terrestriality. This wealth of tetrapods from Tournaisian localities highlights the potential for discoveries elsewhere.

The term “Romer’s Gap” was coined[1,2] for a hiatus of approximately 25 million years (Myr)[3] in the fossil record of tetrapods from the end-Devonian to the Mid-Mississippian (Viséan). Following the end-Devonian, the earliest terrestrial tetrapod fauna was known from the early Brigantian (late Viséan) locality of East Kirkton near Bathgate,

48 Scotland[4,5]. By that time, tetrapods were ecologically diverse, and were terrestrially
49 capable. With five or fewer digits, some had gracile limbs[6,7], unlike the polydactylous
50 predominantly aquatic fish-like tetrapods of the Late Devonian[8]. Fossils representing
51 transitional morphologies between these disparate forms was almost entirely lacking,
52 limiting both understanding of the acquisition of terrestrial characteristics and the
53 relationships between the diverse mid-Carboniferous taxa. Alternative hypotheses to
54 explain the hiatus have included a low oxygen regime[9] or lack of successful collecting
55 in Tournaisian strata[2].

56 Although isolated tetrapod limb bones, girdle elements, and trackways are
57 known from the Tournaisian of the Horton Bluff Formation at Blue Beach, Nova
58 Scotia[10,11], only a small fraction has been fully described[12]. The only other Tournaisian
59 tetrapod material was the articulated skeleton of *Pederpes finneyae*, from the
60 Tournaisian Ballagan Formation near Dumbarton, western Scotland[13,14]. More recently,
61 new taxa from this formation in the Borders Region of Scotland were reported[2], but
62 further collecting from five localities (**Supplementary Fig. 1**) has since produced more
63 data about the fauna, its environment, and climatic conditions.

64 Our analysis shows that the Tournaisian included a rich and diverse assemblage
65 of taxa which included close relatives of some Devonian forms on the tetrapod stem, and
66 basal members of the amphibian stem. We diagnose, name and analyse five taxa (Figs 1-
67 5), and summarize at least seven others that are distinct but undiagnosable at present
68 **(**Fig. 6, **Supplementary Figs 2-6)**.

69 Tetrapods occupied a juxtaposed mosaic of microhabitats including ponds,
70 swamps, streams, and floodplains with highly variable salinity and water levels in a

sharply contrasting seasonal climate. Their fossils are most closely associated with palaeosols and the overlying sandy siltstones. These indicate exposed and vegetated land surfaces that were then flooded[15,16] (**Supplementary Fig 7**). This varied environment persisted over the 12 million years of the Tournaisian[3]. We show that atmospheric oxygen levels were stable across the Devonian/Carboniferous boundary, and did not therefore compromise terrestrial faunal life (contra ref 9).

Differential diagnoses below give the characters in which each differs from all other tetrapods in its combination of autapomorphic and derived (relative to Devonian taxa) characters.

This published work and the nomenclatural act it contains have been registered in Zoobank: http://www.zoobank.org:pub:4BFFB544-7B0B-4F2F-80EC-11226C0FDAAB

Tetrapoda Goodrich, 1930 indet.

Perittodus apsconditus gen. et sp. nov. Clack and Smithson T.R. Fig. 1 e-g. Smithson et al., 2012 (fig. 4), new taxon A.

LSID. urn:lsid:zoobank.org:act 69DB72E5-F9BD-49C6-B471-CD8E03767732

Etymology. Genus from *perittos* (Greek) 'odd' and *odus* (Greek) 'tooth' referring to the unusual dentition of the mandible. Species from *apsconditus* (Latin) 'covert, disguised, hidden, secret or concealed', referring to the fact that key parts were only discovered by micro-CT scanning.

Holotype. UMZC 2011.7.2 a and b. Cheek region of skull, lower jaw, and postcranial elements in part and counterpart.

Locality and Horizon. Willie's Hole, Whiteadder Water near Chirnside. Ballagan Formation. Early mid Tournaisian.

Diagnosis. Autapomorphies: unique adsymphysial and coronoid dentition – adsymphysial with two tusks and at least two smaller teeth, anterior coronoid with two

or three larger tusks, middle coronoid with two larger and two or three smaller teeth, posterior coronoid row of small teeth; lozenge-shaped dorsal scales bearing concentric ridges centred close to one edge nearer to one end. Derived characters: deeply excavated jugal with narrow suborbital bar; lateral line an open groove on jugal.

Plesiomorphies & characters of uncertain polarity: No mesial lamina of postspenial (state of angular not known); 35 dentary teeth including spaces; 29 maxillary teeth including spaces; room for possibly 6 teeth on premaxilla; marinal teeth similar in size; short broad phalanges, rounded unguals longer than wide with ventral ridge.

Attributed specimen. UMZC 2016.1. Isolated dentary and adsymphysial (in micro-CT scan) from Burnmouth Ross end cliffs, 373.95 m above the base of the Ballagan Formation. Mid Tournaisian.

Remarks: Lower jaw length 68 mm. Maxilla of holotype visible in micro-CT scan. UMZC 2016.1 is almost identical in size and dentition to the holotype. The pattern is most similar to but not identical with, that of the Devonian taxon *Ymeria*[17]. A distinct denticulated ridge on the prearticular is set off from the remainder of the bone by a ventral groove. Radius and ulna are of approximately equal length. A partial ischium reveals similarities to that of *Baphetes*[18].

Koilops herma gen. et sp. nov. Clack and Smithson T.R. Fig. 1 a-b.

Smithson et al., 2012 (fig. 2C), ‘probable new taxon’.

LSID. urn:lsid:zoobank.org:act 8C43E66A-3822-49B4-B3B5-E43C79FA9C70

Etymology. Genus from *koilos* (Greek) ‘hollow or empty’, and *ops* (Greek) ‘face’, referring to the skull mainly preserved as natural mould. Species from *herma* (Greek) ‘boundary marker, cairn, pile of stones’. The specimen, from the Borders Region of Scotland, has transitional morphology between Devonian and Carboniferous tetrapods.

Holotype. NMS G. 2013.39/14. Isolated skull mainly as a natural mould.

Locality and Horizon. Willie's Hole, Whiteadder Water near Chirnside. Ballagan Formation. Early mid Tournaisian.

Diagnosis. Autapomorphies: fine irregular dermal ornament with conspicuous curved ridges around the parietal foramen and larger pustular ornament anterior to parietal foramen. Derived characters: deeply excavated jugal with narrow suborbital bar; large parietal foramen.

Plesiomorphies & characters of uncertain polarity: Orbit oval with slight anterior embayment; prefrontal-postfrontal contact narrow, anterior to orbit mid-length; about 8 premaxillary teeth recurved, sharply pointed, ridged towards base; closed palate, denticulated pterygoid; vomers bearing tusks and smaller teeth, at least four moderately large teeth on palatine; short rounded snout, only slightly longer than maximum orbit length.

Remarks. Skull length 80 mm. The dermal bones are robust and well integrated so the individual was almost certainly not a juvenile.

Ossirarus kierani gen. et sp. nov. Clack and Smithson T.R. Fig. 2.

LSID. urn:lsid:zoobank.org:act FC9FAB5C-CC3E-4D0D-B7D7-8030FBAA4F0C

Etymology. Genus from *ossi* (Latin) 'bones' and *rarus* (Latin) 'scattered or rare.' Specific name to honour Oliver and Betty Kieran, representing the Burnmouth community, who have supported us and encouraged local interest and co-operation.

Holotype. UMZC 2016.3. A single block containing scattered skull and postcranial remains.

Locality and Horizon. Burnmouth Ross end cliffs, 340.5 m above the base of the Ballagan Formation. Mid Tournaisian.

Diagnosis. Autapomorphies: tabular elongate triangle forming a conspicuous tabular horn with a convex lateral margin. Derived character: tabular-parietal contact; exoccipital separate from basioccipital.

Plesiomorphies & characters of uncertain polarity: Jugal with extensive posterior component, with anteriorly placed shallow contribution to orbit; lozenge-shaped interclavicle; humerus with elongate and oblique pectoralis process comparable with the ventral humeral ridge of elpistostegalians and *Acanthostega*; multipartite vertebrae with diplospondylous widely notochordal centra and neural arches as unfused bilateral halves.

Remarks: Estimated skull length 50 mm based on comparisons with *Acanthostega*, *Ichthyostega* and *Greererpeton*[19-21]. The primitive jugal morphology, with an elongated postorbital region and an anteriorly placed orbital margin contributing less than 25% of the orbit margin, is similar to that in *Acanthostega*[19] and *Ichthyostega*[20]. The tabular has an elongated posterior process, but its lateral margin does not show an embayment for a spiracular notch. The bones are robust, with well defined overlap areas for interdigitating sutures. Though disarticulated, these suggest that the individual was not a juvenile. The specimen shows the earliest known occurrence of a separate exoccipital.

Diploradus austiumensis gen. et sp. nov. Clack and Smithson T.R. Fig. 3.

LSID. urn:lsid:zoobank.org:act 268DDD4F-289D-4F83-8172-1A18A1007B7C

Etymology. Genus from *diplo* (Greek) ‘double’ and *radus* (Greek) ‘row’ referring to the double coronoid tooth row. Species from *austium* (Latin) ‘mouth of a river or stream’ referring to Burnmouth.

Holotype. UMZC 2015.55.4. Small disrupted skull with lower jaw, palate and skull roofing bones.

Locality and Horizon. Burnmouth Ross end cliffs, 373.95 m above the base of the Ballagan Formation. Mid Tournaisian.

Diagnosis. Autapomorphies: lower jaw with irregular double row of denticles along the coronoids; around 51 dentary teeth and spaces, with enlarged tusk at position 3 and the largest teeth in positions 8-13; parietals short, pineal foramen anteriorly placed; ?narrow curved pre- and postfrontals. Derived characters: deeply excavated jugal with narrow suborbital bar; parasphenoid with broad, flattened posterior portion with lateral wings, earliest known occurrence of a parasphenoid crossing the ventral cranial fissure, cultriform process flat, narrow.

Attributed specimen. UMZC 2016.4 a and b. The anterior end of a mandible from 341 m above the base of the Ballagan formation at Burnmouth.

Plesiomorphies & characters of uncertain polarity: Unsutured junction between prearticular and splenial series; adductor fossa dorsally placed; adsymphysial plate possibly lacking dentition; closed, denticulated palate; broad pterygoid, quadrate ramus narrow with vertically orientated medial ascending lamina; ossified hyobranchial elements; maxilla and premaxilla with spaces for 35 and 10-12 teeth respectively; maxilla-premaxilla contact narrow, lacking interdigitations; dermal ornament with low profile, irregular on skull table, ridged on squamosal and quadratojugal.

Remarks. Lower jaw length 30 mm, superficially resembling that of *Sigournea*[22], although a relationship is not supported by cladistic analysis. The thinness of the bones and their distribution suggest a juvenile.

Aytonerpeton microps gen. et sp. nov. Otoo, Clack and Smithson T.R. Fig. 4.

LSID. urn:lsid:zoobank.org:act E1E094A8-FAC0-4A2A-A13D-487D7775FBE1

Etymology. Genus name from Ayton, the parish in the Scottish Borders from which the specimen came, and *erpeton* (Greek) 'crawler' or 'creeping one'. Species name from *micro* (Greek) 'small' and *ops* (Greek) 'face'.

Holotype. UMZC 2015.55.8. Partial skull and scattered postcrania visible only in micro-CT scan (**Supplementary Movie Files**)

Locality and Horizon. Burnmouth Ross end shore exposure, 340.6 m above the base of the Ballagan Formation. Mid Tournaisian.

Diagnosis. Autapomorphies: two enlarged premaxillary teeth plus one large tooth space at posterior end of premaxilla; 5 teeth on premaxilla; adsymphysial with a single tooth; coronoids apparently lacking shagreen; L-shaped lacrimal; vomer with at least one tooth, palatine with one large fang but lacking smaller teeth; ectopterygoid with at least two teeth and possible smaller teeth. Derived characters shared with colosteids: course of lateral line on maxilla and nasal; dentary teeth larger and fewer than upper marginal teeth; single large Meckelian fenestra; interpterygoid vacuities longer than wide; single large parasymphysial fang on dentary; ilium with a single strap-shaped iliac process.

Remarks. Reconstructed skull length about 50 mm. Other distinguishing features: short snout, approximately similar in length to orbit diameter; naris and choana both very large relative to skull size – relatively larger than in *Greererpeton*. The enlarged premaxillary teeth prefigure those of more derived colosteids[e.g.21], but the dentary lacks the corresponding reciprocal notch. This appears an early expression of a feature that becomes more elaborate in later taxa. All coronoids bear at least one tooth. Some colosteids lack coronoid teeth, and instead bear shagreen, a variable condition among individuals[23]. The small size of the skull but the strong integration of the lower jaw bones suggest a subadult or adult in which case the large orbit is unlikely to be a

219 juvenile feature (c.f. juvenile *Greererpeton* CMNH 11095[24]). Its gracile limbs,
220 metapodial bones and phalanges resemble *Colosteus* rather than *Greererpeton*.
221 Clavicular ornament is similar to that of other colosteids[25,26]. The single iliac process is
222 shared with other colosteids and with temnospondyls.The earliest known occurrence of
223 this feature.
224
225 **Results**
226 **Cladistic Analysis**
227 We performed parsimony and Bayesian analyses of a new data matrix (**Supplementary**
228 **Data Character list and Data matrix**) incorporating the new tetrapods. No taxon could
229 be safely deleted[27]. Parsimony with all characters unordered and equally weighted
230 produced 4718 shortest trees, a poorly resolved strict consensus (Fig. 5, **Supplementary**
231 **Fig. 8**), and moderate branch support.
232 Four parsimony analyses with implied weighting, each using a different value (3,
233 4, 5, 10) of the concavity constant K[28] produced many fewer trees (Fig. 5a, b), with
234 novel topologies and increased stability for most of the new taxa. In these analyses, the
235 relative positions of *Ossirarus*, *Perittodus*, and *Diploradus* remain unaltered (**Methods**
236 **and Supplementary Fig. 8**). Except in the analysis with K=10, *Koilops* and
237 *Aytonerpeton* emerge as stem amphibians[29-31, but see 32,33] with *Aytonerpeton* close to
238 *Tulerpeton*+colosteids. With characters reweighted by their rescaled consistency index,
239 all new taxa emerge as stem tetrapods.
240 We also performed a Bayesian analysis (Fig. 5c). The results were largely similar
241 to the parsimony analysis, except for the position of *Ossirarus*. In the Bayesian analysis,
242 *Ossirarus* appears as a stem amniote, whilst *Perittodus*, *Diploradus*, *Koilops*, and

Aytonerpeton are stem tetrapods.

Despite inconsistencies, these results imply a substantial reshuffling of the branching sequence of Carboniferous stem tetrapods relative to previous studies[29-33], with interspersed Carboniferous and Devonian taxa pointing to a more ramified stem of tetrapod diversification. If corroborated by further evidence, a firmer placement of *Aytonerpeton* and *Koilops* within crown tetrapods would suggest a deep split between stem amphibians and stem amniotes within the Tournaisian..

Geology and Environment

The Ballagan Formation (Inverclyde Group) underlies much of the Midland Valley of Scotland and the northern margin of the Northumberland Basin. At Burnmouth the vertically dipping strata probably span the entire Tournaisian[2,34]. Environmental interpretation was based on a 490 m core from a borehole through the formation, a complete logged succession at centimetre scale intervals through 520 m at Burnmouth, and an 8 m section at Willie's Hole (Fig. 6, **Methods and Supplementary Fig. 7**).

Perittodus apsconditus occurs within a 6 cm thick laminated grey siltstone[16] that contains a network of cracks filled with sandy siltstone identical to that of the overlying bed. Occurring within laminated siltstones, this may record an autochthonous lake dweller. Associated fossils comprise plants, actinopterygians, myriapods and ostracods. *Koilops* occurs within a unit comprising four beds of alternating black and green siltstone in which abundant palaeosol clasts indicate erosion and transport of land-surface sediment during flooding events.

Diploradus occurs in a 40 cm thick, bedded, black sandy siltstone that lies between pedogenically modified grey siltstones. Associated fossils comprise fish scales, abundant plant fragments, megaspores, and shrimp and scorpion cuticle.

Ossirarus and *Aytonerpeton* occur within a complex 15 cm thick grey-black sandy siltstone that overlies a gleyed palaeosol and grades upwards into a laminated grey siltstone with brecciation cracks (Fig. 6, **Methods and Supplementary Fig. 7**). *Ossirarus* occurred just above the palaeosol in a light grey clay-rich sandy siltstone, whereas *Aytonerpeton* occurred within an overlying black sandy siltstone with abundant plant material. Associated fauna comprise abundant plants, megaspores, unusually abundant rhizodont bones and scales, actinopterygians, chondrichthyans (*Ageleodus, Gyracanthus*), dipnoans, eurypterids and ostracods.

An association between wetland palaeosols and tetrapod-bearing facies has emerged from our studies, significant because those horizons indicate a vegetated land surface (Fig. 6)[15,16]. The flood-plain environments of semi-permanent water bodies, marsh, river banks and areas of dry land with trees were laid down at a time of change in the land plant flora of the Mississippian following the end-Devonian extinctions. The new flora initiated a change in fluvial and floodplain architecture[35-37]. Progymnosperms had been almost eliminated in the extinctions, but thickets and forests were re-established in the early-mid Tournaisian with lycopods as the dominant flora. At Burnmouth many beds with abundant spores of the creeping lycopod *Oxroadia* include tetrapods. Terrestrial ground-dwelling arthropods, such as myriapods and scorpions fossils of which have been found at Burnmouth and at Willie's Hole, formed a possible food supply for tetrapods..

Atmospheric oxygen levels in the Tournaisian

To address the low oxygen hypothesis[9] we examined fossil charcoal (fusinite) in the Ballagan Formation to compare atmospheric oxygen levels in the Tournaisian with the Late Devonian and later Mississippian.

Charcoal, either as microscopic dispersed organic matter (DOM) or visible in hand specimens is relatively common at Burnmouth and Willie's Hole. Although charcoal is reported from the Tournaisian Horton Bluff Formation, Nova Scotia[38] as indicating O_2 concentrations above 16%, no quantitative study to validate this result has been undertaken.

We analysed DOM from 73 rock samples from Burnmouth shore and Willie's Hole. For comparison with wildfire activity before and after Romer's Gap, we also analysed 42 samples from the Viséan of East Fife, Scotland (Strathclyde Group) and 9 samples from the Famennian of Greenland (Stensiö Bjerg Formation) (**Supplementary Fig. 9 and Supplementary Table 1**). All were found to contain fusinite, with a mean abundance relative to total phytoclasts of 2.2%, 2.3% and 2.6% for the Famennian, Tournaisian and Viséan, respectively. We also analysed 12 samples from Willie's Hole which had a mean value of 2.0% (**Supplementary Table 1**). Not only do these results mean that fire activity persisted through Romer's Gap and indicate that atmospheric O_2 did not fall below 16%, but also that there was no significant change in charcoal production compared with the Famennian and Viséan (**Supplementary Fig. 9**). This strongly suggests that atmospheric O_2 was stable across this time interval, directly refuting hypoxia[9] as an explanation for Romer's Gap.

Discussion

313 Although an extinction event at the end of the Devonian saw the demise of many archaic
314 fish groups[39], our studies provide new perspectives on the recovery and diversification
315 of surviving groups, which went on to found the basis of modern vertebrate
316 diversity[40,41].

317 The new tetrapods show no close relationship to each other, exhibiting different
318 combinations of plesiomorphic and derived characters. Some taxa cluster with Devonian
319 forms, suggesting a possible relict fauna, whereas others appear more crownward, even
320 clustering near the base of the crown group. They imply an early radiation of tetrapods
321 during the Tournaisian, and at the same time, suggest a blurring of the Devonian-
322 Carboniferous (D-C) boundary in respect of tetrapod evolution, a feature also noted in
323 tetrapod remains from Nova Scotia[12].

324 If confirmed, our results imply a deep split between stem amphibians and stem
325 amniotes in the earliest Carboniferous. This accords with most molecular dates for the
326 split that place it at an average of 355 Ma[42,43] a date only 4 Ma after the end-Devonian.
327 It suggests that the origin of the tetrapod crown group occurred soon after the extinction
328 event as tetrapods began to recover. Their radiation into a range of new taxa parallels
329 that of lungfish[40] and chondrichthyans[41] as they adapted to a post-extinction world.

330 The occurrence of probable plesiomorphic members of the Crassigyrinidae[2] and
331 Colosteidae indicates an inception 20-24 Myr earlier than the Late Mississippian as
332 previously considered[44]. Other tetrapod material of uncertain attribution are distinct and
333 increase known tetrapod diversity in the Tournaisian (Fig. 6 and **Supplementary Figs 2-**
334 **6**).

The preponderance of small animals throughout the sequence is unusual, notably a very small tetrapod in a horizon 33 m above the D-C boundary, around 1 Myr after the extinction event (Fig. 6). None of the five taxa described above has a skull length of more than 80 mm. This could indicate preservational or collector bias, but they occur throughout different lithologies, horizons and localities (Fig. 6 and **Supplementary Figs 2-6**). Larger tetrapod taxa are found at Willie's Hole, about one quarter of the way up the sequence, probably representing about 3 or 4 Myr above the D-C boundary. Larger sizes seem to have appeared relatively rapidly in the Tournaisian, as also documented by trackways[38] and challenge suggestions of a prolonged period of reduced body size in vertebrates following the DC extinction event[45].

The tetrapods of the Ballagan Formation lived in a mosaic of floodplain environments. Some were under water for long periods, others alternated between land surface and standing water. A recent study of the development of *Polypterus* shows how early in life, their skeletons can be differentially modified in response to exposure to water-based or land-based conditions[46]. Such skeletal flexibility might have contributed to the origin of tetrapod terrestrial morphology in the varied environments of the Ballagan Formation.

The wealth and diversity of tetrapod taxa from the Tournaisian refutes the proposal of depauperate Tournaisian stage, and our charcoal studies show that atmospheric oxygen levels, stable from the Famennian to the Viséan, were not a causal factor for the apparent gap. We emphasise the importance of exploring or re-exploring non-marine Tournaisian sites elsewhere in the world, and examining previously overlooked lithologies.

References

1. Coates, M. I & Clack, J. A. Romer's Gap – tetrapod origins and terrestriality. *Bull. Mus. Nat. Hist. Nat.* **17**, 373-388 (1995)
2. Smithson, T. R., Wood, S. P., Marshall, J. E. A. & Clack, J. A. Earliest Carboniferous tetrapod and arthropod faunas from Scotland populate Romer's Gap. *Proc. Natl. Acad. Sci. USA* **109,** 4532-4537 (2012)
3. Cohen, K.M., Finney, S.C., Gibbard, P.L. & Fan, J.-X. The International Chronostratigraphical Chart, *Episodes* **36**, 199-204 (2013) http://stratigraphy.org/ICSchart/ChronostratChart2016-04.pdf
4. Wood, S. P., Panchen, A. L. & Smithson, T. R. A terrestrial fauna from the Scottish Lower Carboniferous. *Nature* **314**, 355-356 (1985)
5. Rolfe, W. D. I., Clarkson, E. N. K. & Panchen, A. L. (Eds). Volcanism and early terrestrial biotas. *Trans. R. Soc. Edinb. Earth Sci.* **84**, (1994)
6. Milner, A. R. & Sequeira, S. E. K. The temnospondyl amphibians from the Viséan of East Kirkton, West Lothian, Scotland. *Trans. R. Soc. Edinb. Earth Sci.* **84**, 331-362 (1994)
7. Smithson, T. R., Carroll, R. L., Panchen, A. L. & Andrews, S. M. *Westlothiana lizziae* from the Viséan of East Kirkton, West Lothian, Scotland. *Trans. R. Soc. Edinb. Earth Sci.* **84**, 417-431 (1994)
8. Clack, J. A. *Gaining Ground: The origin and evolution of tetrapods.* 2nd Ed. 1-523. (Indiana Univ. Press, 2012)
9. Ward, P. D., Labandeira, C., Laurin, M. & Berner, R. A. Confirmation of Romer's Gap as a low oxygen interval constraining the timing of initial arthropod and vertebrate terrestrialisation. *Proc. Natl. Acad. Sci. USA* **103**, 16818-16822 (2006)

10. Carroll, R. L., Belt, E. S., Dineley, D. L., Baird, D. & McGregor, D. C.Excursion A59, Vertebrate palaeontology of Eastern Canada. *24th International Geological Congress, Montreal* (1972)

11. Clack, J. A. & Carroll, R. L. in *Amphibian Biology, Vol. 4: Palaeontolog* (eds Heatwole, H. & Carroll, R. L.) 1030-1043 (Surrey Beatty, 2000)

12. Anderson, J. S., Smithson, T. R., Mansky, C. F., Meyer, T. & Clack, J. A. A diverse tetrapod fauna at the base of Romer's Gap. *Plos One* DOI:10.1371/journal.pone.0125446 (2015)

13. Clack, J. A. An early tetrapod from 'Romer's Gap'. *Nature* **418**, 72-76 (2002)

14. Clack, J. A. & Finney, S. M. *Pederpes finneyae*, an articulated tetrapod from the Tournaisian of western Scotland. *J. Syst. Palaeont*. **2**, 311-346 (2005)

15. Kearsey, T. I., Bennett, C. E., Millward, D., Davies, S. J., Gowing, C. J. B., Kemp, S. J., Leng, M. L., Marshall, J. E. A., Browne, M. A. E. The terrestrial landscapes of tetrapod evolution in earliest Carboniferous seasonal wetlands of SE Scotland. *Palaeogeogr, Palaeoclim, Palaeoeco* **457**, 52-69 doi.org/10.1016/j.palaeo.2016.05.033 (2016)

16. Bennett, C. E., Kearsey, T. I., Davies, S. J., Millward, D. Clack, J. A., Smithson,T. R. & Marshall, J. E. A. Early Mississippian sandy siltstones preserve rare vertebrate fossils in seasonal flooding episodes. *Sediment.* "Enhanced Article"; doi: 10.1111/sed.12280 (2016)

17. Clack, J.A., Ahlberg P.E., Blom H., & Finney S.M. A new genus of Devonian tetrapod from East Greenland, with new information on the lower jaw of *Ichthyostega*. *Palaeont.* **55**, 73-86 (2012)

18. Milner, A. C. & Lindsay, W. Postcranial remains of *Baphetes* and their bearing on the relationships of the Baphetidae (= Loxommatidae). *Zoo. J. Linn. Soc.* **122**, 211-235 (1998)

19. Clack, J. A. The dermal skull roof of *Acanthostega*, an early tetrapod from the Late Devonian. *Trans. R. Soc. Edinb. Earth Sci.* **93**, 17-33 (2002)

20. Jarvik, E. The Devonian tetrapod *Ichthyostega*. *Fossils and Strata* **40**, 1-206 (1996)

21. Smithson, T. R. The cranial morphology of *Greererpeton burkemorani* (Amphibia: Temnospondyli). *Zoo. J. Linn. Soc.* **76**, 29-90 (1982)

22. Lombard, R. E. & Bolt, J. R. *Sigournea multidentata*, a new stem tetrapod from the Upper Mississippian of Iowa, USA. *J. Palaeont*. **80,** 717-725 (2006)

23. Bolt J. R. & Lombard, R. E. The mandible of the primitive tetrapod *Greererpeton*, and the early evolution of the tetrapod lower jaw. *J. Paleont.* **75**, 1016-1042 (2001)

24. Godfrey, S. J. Ontogenetic changes in the skull of the Carboniferous tetrapod *Greererpeton burkemorani* Romer 1969. *Phil. Trans. Roy. Soc. Lond. B* **323**, 135-153 (1989a)

25. Hook, R. W. *Colosteus scutellatus* (Newberry) a primitive temnospondyl amphibian from the Middle Pennsylvanian of Linton, Ohio. *Am. Mus.Novit.* **2770**, 1-41 (1983)

26. Godfrey, S. J. The postcranial skeletal anatomy of the Carboniferous tetrapod *Greererpeton burkemorani* Romer 1969. *Phil. Trans. Roy. Soc. Lond. B* **323**, 75-133 (1989b)

27. Wilkinson, M. Coping with abundant missing entries in phylogenetic inference using parsimony. *Syst. Biol.* **44**, 501-514 (1995)

28. Goloboff, P. A. Estimating character weights during tree search. *Cladistics* **9**, 83-89 (1993)

29. Ruta, M., Coates, M. I. & Quicke, D. L. J. Early tetrapod relationships revisited. *Biol. Rev.* **78**, 251-345 (2003)

30. Ruta, M. & Clack, J. A. A review of *Silvanerpeton miripedes*, a stem amniote from the Lower Carboniferous of East Kirkton, West Lothian, Scotland. *Trans. R. Soc. Edinb. Earth Sci.* **97**, 31-63 (2006)

31. Klembara J., Clack, J. A. & Milner A. R. Cranial anatomy, ontogeny, and relationships of the Late Carboniferous tetrapod *Gephyrostegus bohemicus* Jaekel, 1902. *J. Vert. Pal.* **34**, 774-792. (2014).

32. Laurin, M. The evolution of body size, Cope's rule and the origin of amniotes. *Syst. Biol.* **53**, 594-622 (2004).

33. Marjanović, D. & Laurin, M. The origin(s) of extant amphibians: a review with emphasis on the "lepospondyl hypothesis". *Geodiversitas* **35**, 207-272. (2013)

34. Greig, D. C. *Geology of the Eyemouth district*. Memoir of the British Geological Survey, Sheet 34. (1988)

35. Garcia, W.J., Storrs, G.W. & Greb, S.F. The Hancock County tetrapod locality: A new Mississippian (Chesterian) wetlands fauna from western Kentucky (USA). *Geol. Soc. Am. Spec. Papers* **399**, 155-167 (2006)

36. Davies, N. S. & Gibling, M. R. The sedimentary record of Carboniferous rivers: Continuing influence of land plant evolution on alluvial processes and Palaeozoic ecosystems. *Earth-Sci. Rev.* **120**, 40-79 (2013)

37. Corenblit, D., Davies, N. S., Steiger, J., Gibling, M. R. & Bornette, G. Considering river structure and stability in the light of evolution: feedbacks between riparian vegetation and hydrogeomorphology. *Earth Surf. Proc. Land.*

40, 189-207 (2015)

38. Mansky, C. F. & Lucas, S. G. Romer's Gap revisited: continental assemblages and ichno-assemblages from the basal Carboniferous of Blue Beach, Nova Scotia, Canada. *Bull. New. Mex. Mus. Nat. Hist.* **60**, 244-273 (2013).
39. Sallan, L. C. & Coates, M. I. End-Devonian extinction and a bottleneck in the early evolution of modern jawed vertebrates. *Proc. Nat. Acad. Sci. USA* **107,** 10131-10135 (2010)
40. Smithson, T. R., Richards, K. R. & Clack, J. A. Lungfish diversity in Romer's Gap: reaction to the end-Devonian extinction. *Palaeont.* **59**, 29-44 (2016).
41. Richards, K. R., Sherwin, J. E., Smithson, T. R., Bennion, R. F., Davies, S. J., Marshall, J. E. A. & Clack, J. A. A new fauna of early Carboniferous chondrichthyans from the Scottish Borders. http://www.palass.org/meetings-events/annual-meeting/2015/annual-meeting-2015-cardiff-poster-abstracts (2015)
42. Hedges, S. B., Marin, J., Suleski, M., Paymer, M. & Kumar, S. Tree of Life reveals clock-like speciation and diversification. *Mol. Biol. Evol.* **32**, 835-845 (2015)
43. Kumar S. & Hedges S. B. TimeTree2: species divergence times on the iPhone. *Bioinformatics* 27:2023-2024 www.timetree.org (2011)
44. Clack, J. A., Witzmann, F., Snyder D., and Müller, J. 2012 A colosteid-like early tetrapod from the St. Louis Limestone (Early Carboniferous, Meramecian), St. Louis, Missouri, USA. *Fieldiana Life Earth Sci.***5**, 17-39.
45. Sallan L. C. & Gallimberti, A. K. Body-size reduction in vertebrates following the end-Devonian mass extinction. *Science* **350**, 812-815 (2015)

46. Standen, E. M., Du, T. Y. & Larsson, C. E. Developmental plasticity and the origin of tetrapods. *Nature* **513**, 54-58. (2014) doi:10.1038/nature13708

47. Ahlberg, P. E. and Clack, J. A. Lower jaws, lower tetrapods: a review based on the Devonian tetrapod *Acanthostega*. *Trans. R. Soc. Edinb.* **89**, 11-46 (1998)

48. Clack, J. A. The Scottish Carboniferous tetrapod *Crassigyrinus scoticus* (Lydekker) - cranial anatomy and relationships. *Trans. R. Soc. Edinb.* **88**, 127-142. (1998)

49. Goloboff, P. A., Farris, J. S., & Nixon, K. C. TNT, a free program for phylogenetic analysis. *Cladistics* **24**, 1-13 (2008)

50. Carpenter, D. K., Falcon-Lang, H. J., Benton, M. J., & Henderson, E. Carboniferous (Tournaisian) fish assemblages from the Isle of Bute, Scotland: systematics and palaeoecology. *Palaeont.* **57**, 1215-1240 (2014)

51. Friedman, M. & Sallan, L. C. Five hundred million years of extinction and recovery: a Phanerozoic survey of large-scale diversity patterns in fishes. *Palaeont.* **55**, 707-742 (2012)

52. Andrews, J. E., Turner, M. S., Nabi, G. & Spiro, B. The anatomy of an early Dinantian terraced floodplain: palaeo-environment and early diagenesis. *Sediment.* **38**, 271-287 (1991)

53. Turner, M.S. *Geochemistry and diagenesis of basal Carboniferous dolostones from southern Scotland* (Unpublished Ph.D. thesis, University of East Anglia, 1991)

54. Belt, E. S., Freshney, E. C. & Read, W. A. Sedimentology of Carboniferous cementstone facies, British Isles and Eastern Canada. *J. Geol.* **75**, 711-721. (1967)

55. Scott, W. B. *The sedimentology of the cementstone group in the Tweed basin:*

Burnmouth and the Merse of Berwick. (Unpublished PhD Thesis, Sunderland Polytechnic 1971)

56. Scott, W. B. Nodular carbonates in the Lower Carboniferous, Cementstone Group of the Tweed Embayment, Berwickshire: evidence for a former sulphate evaporite facies. *Scot. J. Geol.* **22**, 325-345 (1986)
57. Barnet, A. J., Wright, V. P. & Crowley, S. F. Recognition and significance of paludal dolomites: Late Mississippian, Kentucky, USA. *Interl Assn Sediment. Spec. Publ.* **45**, 477-500 (2012)
58. Muchez, P. & Viaene, W. Dolocretes from the Lower Carboniferous of the Campine-Brabant Basin, Belgium. *Pedologie* **37**, 187–202 (1987)
59. Searl, A. Pedogenic dolomites from the Oolite Group (Lower Carboniferous),South Wales. *Geol. J.* **23**,157–169 (1988)
60. Vanstone, S. D. Early Carboniferous (Mississippian) palaeosols from southwest Britain: influence of climatic change on soil development. *J. Sediment. Petrol.* **61**, 445–457 (1991)
61. Wright, V. P., Vanstone, S. D. & Marshall, J. D. Contrasting flooding histories of Mississippian carbonate platforms revealed by marine alteration effects in palaeosols. *Sedimentology* **44**, 825–842 (1997)
62. Wood, G., Gabriel, A.M. & Lawson, J.C. Palynological techniques –processing and microscopy. 29–50 in: *Palynology: Principles and Applications, Volume 1. Principles*. (eds) Jansonius, J. and McGregor, D. C. (American Association of Stratigraphic Palynologists Foundation, Texas, 1996).
63. American Society for Testing and Materials (ASTM). D2799 - 13. Standard test method for microscopical determination of the maceral composition of coal. in: *Annual book of ASTM standards section 5 – Petroleum products, lubricants, and*

their fossil fuels. Volume 05.06 Gaseous Fuels; Coal and Coke; Bioenergy and Industrial Chemicals from Biomass. (West Conshohocken, PA, ASTM International. DOI**:** 10.1520/D2799-13 http://www.astm.org/Standards/D2799.htm (2013)

64. Hansen, K. W. & Wallmann, K. Cretaceous and Cenozoic evolution of seawater composition, atmospheric O_2 and CO_2: A model perspective. *Am. J. Sci.* **303**, 94–148 (2003).
65. Bergman, N. M., Lenton, T. M. & Watson, A. J. COPSE: a new model of biogeochemical cycling over Phanerozoic time. *Am. J. Sci.* **304**, 397–437 (2004).
66. Arvidson, R.S., Mackenzie, F.T. & Guidry, M. Magic: A Phanerozoic model for the geochemical cycling of major rock-forming components. *Am. J. Sci.* **306**, 135–190 (2006).
67. Berner, R. A. GEOCARBSULF: A combined model for Phanerozoic atmospheric O_2 and CO_2. *Geochim. Cosmochim. Ac.* **70**, 5653–5664 (2006)
68. Berner, R. A. Phanerozoic atmospheric oxygen: new results using the GEOCARBSULF model. *Am. J. Sci.* **309**, 603–606 (2009)
69. Robinson, J. M. Phanerozoic atmospheric reconstructions: a terrestrial perspective. *Palaeogeogr. Palaeoclim. Palaeoecol.* **97**, 51-62 (1991)
70. Scott, A. J. & Glasspool, I. J. The diversification of Paleozoic fire systems and fluctuations in atmospheric oxygen concentration. *Proc. Nat. Acad. Sci. USA* **103,** 10861-10865 (2006)
71. Glasspool, I. J., & Scott, A. C. Phanerozoic concentrations of atmospheric oxygen reconstructed from sedimentary charcoal. *Nature Geoscience.* 3, 627-630 (2010)

72. Glasspool, I. J., Scott, A. C., Waltham, D., Pronina, N. & Shao, L. The impact of fire on the Late Paleozoic Earth system. *Front. Plant Sci.* **6**, 1-13 (2015)

73. Belcher, C. M., Yearsley, J. M., Hadden, R. M., McElwain, J. C. & Guillermo, R. Baseline intrinsic flammability of Earth's ecosystems estimated from paleoatmospheric oxygen over the past 350 million years. *Proc. Nat. Acad. Sci. USA* **107**, 22448-22453 (2010)

74. Tyson, R. V. *Sedimentary organic matter*. 1- 615. Chapman & Hall, London, (1995)

75. Scott, A. J. & Glasspool, I. J. Observations and experiments on the origin and formation of the inertinite group macerals. *Internl J. Coal Petr.*, **70**, 53–66. (2007)

76. Owens, B., McLean, D. and Simpson, K. R. M. Reappraisals of the Mississippian palynostratigraphy of the East Fife coast, Scotland, United Kingdom. *Palynology*, **29**, 23–47 (2005)

77. Forsythe, J. H. and Chisholme, J. I. *The geology of East Fife (explanations of the Fife portion of 'one-inch' geological sheet 41 and part of sheet 49)*. (Her Majesty's Stationary Office, Edinburgh, 284pp. 1977)

78. Stephenson, M. H., Williams, M., Monghan, A. A., Arkley, S., Smith, R. A. Dean, M., Browne, M. A. E. and Leng, M. Palynomorph and ostracod biostratigraphy of the Ballagan Formation, Midland Valley of Scotland, and elucidation of intra-Dinantian unconformities. *Proc. Yorks. Geol. Soc.* **55**, 131–143 (2004)

79. Marshall, J. A. E., Astin, T. R. and Clack, J. A. East Greenland tetrapods are Devonian in age. *Geology*, **27**, 637–640 (1999)

80. Astin, T. R., Marshall, J. E. A., Blom, H. and Berry, C. M. The sedimentary environment of the Late Devonian East Greenland tetrapods. 93 – 109 *in*: Vecoli, M., Clement, G. and Meyer-Berthaud, B. (*eds*.) The terrestrialization process: modelling complex interactions at the biosphere-geosphere interface. Geol. Soc. Lond. Spec. Publ. **339** (2010)

Figure legends

Figure 1. a-b *Koilops herma* gen. et sp. nov. (National Museum of Scotland NMS G. 2013.39/14). **a**, Photograph of specimen, mainly preserved as natural mould. **b,** Interpretive drawing of specimen. **c-g,** *Perritodus apsconditus* gen. et sp. nov. (University Museum of Zoology, Cambridge UMZC 2011.7.2a). **c,** Photograph of main specimen block. **d,** Reconstruction of lower jaw in external view, from scan data and part and counterpart specimens. **e,** Reconstruction of lower jaw in internal view made from scan data and part and counterpart specimens. **f,** Segmented model from scans of lower jaw in internal view. **g,** segmented model from scans of lower jaw in internal view. Colour code in **f**,: orange, dentary; red, adsymphysial plate; turquoise, part of prearticular; yellow, first coronoid; blue, second coronoid; cerise, third coronoid; pink, splenial; violet, angular; purple, prearticular; green, splenial; external bones greyed out. In **g**, green, splenial. Scale bar in **a**, **b**, and **c**, 10 mm. Abbreviations: add foss, adductor fossa; adsymph, adsymphysial; ang, angular; cor, coronoid; dent, dentary; ecto, ectopterygoid; fro, frontal; intemp, intertemporal; jug, jugal; l, left; lac, lacrimal; llc, lateral line canal; max, maxilla; oa, overlap area for pterygoid; pal, palatine; par, parietal; pofr, postfrontal; porb, postorbital; pospl, postsplenial; preart, prearticular;

prefro, prefrontal; premax, premaxilla; psph, parasphenoid; pteryg, pterygoid; quad, quadrate; quj, quadratojugal; surang, surangular; vom, vomer.

Figure 2. *Ossirarus kierani* gen. et sp. nov. (UMZC 2016.3) **a**, Photograph of complete specimen. Leaders point to **b,** Map of skull bones. **c,** Drawing of right tabular, supratemporal and a partial unidentified bone. **d,** Drawing of exoccipital. **e**, Drawing of quadrate. **f,** Photograph enlargement of part of postcranial portion of specimen, **g,** Drawings of left and right parietal bones placed in articulation, **h,** Drawing of jugal and postorbital placed in articulation, **i,** Photograph of jugal. **j,** Photograph enlargement of right humerus. Scale bar in **b** 10 mm, scale bars in **c-j** 5 mm. Abbreviations: clav, clavicle; cleith, cleithrum; exocc, exoccipital; iclav, interclavicle; jug, jugal; par, parietal; porb, postorbital; quad, quadrate; r, right; rad, radius; sutemp, supratemporal; tab, tabular.

Figure 3. *Diploradus austiumensis* gen. et sp. nov. (UMZC 2015.55.4). **a,** Photograph of complete specimen. Scale bar 10 mm, **b,** Map of specimen showing distribution of elements, **c,** Drawing of right maxilla, **d,** Upper, interpretive drawing of specimen; lower, reconstruction of jaw in internal view. **e,** Drawing of parasphenoid. **f,** Drawing of right jugal in internal view. **g,** Drawing of skull table. **h**, Drawing of pterygoid in dorsal view. Scale bars in **b-h**, 5 mm. Abbreviations as for Figures 1 and 2 except for: nat mould popar, natural mould of postparietal.

Figure 4. *Aytonerpeton microps* gen. et sp. nov. (UMZC 2015.55.8). **a,** Still from micro-CT scan of block containing most of the specimen. **b**, Interpretive drawing of right side of skull and palate. **c,** Stills from micro-CT scan of right lower jaw in (upper image)

629 dorsal view and (lower image) mesial view. **d,** Still from micro-CT scan of right palate
630 in approximately ventral view. **e**, Still from micro-CT scan of entire specimen in the
631 main block. Arrows point to elements in **g**. **f,** Enlargement of ilium in lateral (left image)
632 and medial (right image) views. **g**, Elements of hind limb. In **c,** and **d**, note the sutures
633 between pterygoid and marginal palatal bones, and the lower jaw bones, are tightly
634 sutured and difficult to see in the scan. Abbreviations as for Figures 1 and 2, except for:
635 mar Meck fen, margin of Meckelian fenestra; sym, symphysis; septomax, septomaxilla.
636 Scale bars for all except **f** are 10 mm. Scale bar for f is 5 mm.
637
638 **Figure 5.** Three cladograms: two from TNT analysis and one from Bayesian analysis. **a,**
639 Single most parsimonious tree obtained from implied weights search with k=3 (see text
640 and Supplementary Data for details). **b,** strict consensus of four equally parsimonious
641 trees obtained from implied weights search with k=4. **c**, Bayesian analysis tree. See main
642 text, methods, and Supplementary Data for details.
643
644 **Figure 6.** Burmmouth sedimentary log showing palaeosol and tetrapod fossil
645 distribution. Left hand column shows the sedimentary log for Burnmouth with the
646 tetrapod horizons indicated. Right hand column shows the distribution of palaeosols and
647 their thicknesses. Photographs a-g show some of the tetrapod specimens found in
648 addition to those in Figs 1-4.
649 Specimen **a**, an isolated jugal (UMZC 2016.13) from the same bed that yielded the
650 partial *Crassigyrinus*-like jaw in ref 2, horizon approximately 383 m above the base of
651 the Ballagan Formation. This is a thick localized conglomerate lag containing many
652 isolated vertebrate bones, plant remains and charcoal. The shape of the jugal is unique
653 among the tetrapods so far collected from the Ballagan, in its relative contribution to the

654 orbit margin. Probable new taxon 1. Specimens **b-f**, tetrapod specimens from a closely
655 juxtaposed set of horizons beyond the resolution of the log to differentiate, between 340-
656 341m above the base of the Ballagan: **b**, an isolated tetrapod maxilla (UMZC 2016.9); **c**,
657 tetrapod belly scales (UMZC 2016.12) and metapodials/phalanges (UMZC 2016.10, 11);
658 **d,** skull bones and belly scales (UMZC 2016.8); **e**, Micro-CT scan of the two
659 overlapping bones in **d**. They are probable frontal bones of a *Pederpes*-like tetrapod; **f**,
660 partial skull table and postorbitals from slightly above the Burnmouth horizon yielding
661 *Aytonerpeton microps* (UMZC 2016.7). Probable new taxon 2? May be associated with
662 those in **Supplementary Fig. 2**, but not with *Aytonerpeton*. Scale bar 10 mm. (Micro-
663 CT by K. Z. Smithson); **g**, phalanges or metapodials and skull elements of a small
664 tetrapod from Burnmouth (UMZC 2016.5 a, b). Probable new taxon 3. Left hand image,
665 largest elements circled. Right hand image, dentigerous bone near top left corner. Other
666 elements include a probable jugal and rib fragments (not figured). These remains are the
667 earliest post-Devonian tetrapod specimens found in the UK. They come from a horizon
668 approximately 33m above the base of the Ballagan Formation that was probably
669 deposited about 1 Myr after the start of the Carboniferous. Scale bars for all except g are
670 10 mm. Scale for for g is 5 mm. (Photographs by J. A. Clack)
671
672 METHODS
673 Micro-CT data
674 Specimen UMZC 2016.3 *Ossirarus* and NMS G. 2013.39/14 *Koilops* and UMZC
675 2011.7.2a *Perittodus* were prepared mechanically with mounted needle, some matrix
676 was removed from *Ossirarus* with a brush and water, consolidated where necessary with
677 Paraloid B72. Specimens UMZC 2011.7.2a *Perittodus* and UMZC 2015.55.8
678 *Aytonerpeton* were scanned at the Cambridge Tomography Centre with a Nikon

679 XTH225 ST scanner. Scan data:- *Perittodus*: Isotropic voxel size, 0.0444mm.
680 Projections:1080, Filter: 0.25mm Cu, Xray kV:160, Xray µA: 70, Slices:1647.
681 Exposure: 1000, Gain: 24 dB. UMZC 2015.55.8 *Aytonerpeton*: Isotropic voxel size:
682 0.0609mm. Projections: 1080, Filter: None, Xray kV: 120, Xray µA: 125, Slices: 1789,
683 Exposure: 1000, Gain: 24 dB. .
684
685 Cladistic analysis
686 A new database of 46 taxa coded for 214 osteological characters (170 cranial, 43
687 postcranial), and was subjected to maximum parsimony analyses. It was designed to
688 include representative early tetrapods. Characters were drawn up to capture the features
689 of the new taxa as far as possible in the context of the range of early tetrapods available
690 for comparison. Most were drawn from recent analyses [14,29-31,44,47,48]. Some
691 characters were reworded or reformulated and all were independently scored by JAC
692 from personal observation or from the literature. These were checked for accuracy by
693 MR. Characters are arranged in alphabetical order grouped into regions of the anatomy
694 **(Supplementary Data Character list and Data Matrix)**.
695 The data matrix was subjected to maximum parsimony analyses in TNT v. 1.1[49].
696 Several experiments of taxon and character manipulation were carried out, as detailed
697 below, with identical search protocols throughout. Given the size of the matrix, tree
698 searches relied on heuristic algorithms, following a simple series of steps under the
699 'Traditional search' option in the 'Analyze' menu in TNT. Before each search, we
700 modified memory requirements under the 'Memory' option in the 'Settings' menu. One
701 hundred Mbytes of general RAM were allocated, and a total of 50,000 trees were
702 selected as the maximum size of tree space for the exploration of alternative tree
703 topologies. In the initial part of the 'Traditional search' ('Wagner trees' box ticked), we

704 chose 10,000 replicates (random stepwise addition sequences of taxa), keeping a
705 maximum of five trees at the end of each replicate, using the bisection-reconnection
706 algorithm for tree branch swapping, and retaining all trees found at the end of all
707 replicates. A new round of branch swapping was then applied to all trees retained from
708 the initial search ('trees from RAM' box ticked). For each set of experiments, where
709 applicable, we summarized the results in the form of a strict consensus, a 50% majority-
710 rule consensus.

711 Using the search settings expounded above, we carried out three types of
712 parsimony analysis. The first parsimony analysis, employing all taxa and characters
713 from the original matrix, treated all characters as having equal unit weight (default TNT
714 option). The second analysis, again using all taxa and characters, was based on implied
715 character reweighting[28], briefly described as follows. Given a character, its implied
716 weight (W) is given by K / (K + M - O), where M and O represent, respectively, the
717 greatest number of character-state changes and the observed number of character-state
718 changes for that character. The constant of concavity (K) is an integer, the value of
719 which determines the most parsimonious trees as those trees for which W is maximized
720 across all characters. As the selection of K is arbitrary, we experimented with increasing
721 values (K = 3, 4, 5 and 10) (Fig 5, **Supplementary Fig. 8**). We did not report details of
722 searches with other K values, as our goal was to establish whether the Tournaisian taxa
723 showed stable positions within a minimal range of implied weighting increments.
724 However, we ran analyses with values varying between 6 and 10, with mixed outcomes.
725 In some cases, the Tournaisian taxa are heavily reshuffled, in others the branching
726 sequence of other groups revealed implausible arrangements that, we feel, were dictated
727 by varying amounts of homoplasy in the data, although a proper characterization of this
728 phenomenon requires further testing. Topologies with K=10 are reported as an example.

In the third analysis, characters were reweighted by the maximum value (best fit) of their rescaled consistency indexes, such as were obtained from the first analysis.

Statistical branch support was evaluated through character resampling via bootstrap (resampling with replacement; ref.) and jackknife (resampling without replacement, with 33% of characters removed; ref.), using 1000 replicates in each case and collapsing nodes with less than 50% support.

Of all the new Tournaisian taxa, only *Diploradus* appears in a maximum agreement subtree (a taxonomically pruned tree showing only taxa for which all most parsimonious trees agree upon relationships).

As for the implied weighting analysis, we found stable mutual arrangements for most Tournaisian taxa with K = 3, 4 and 5. With K = 10, the branching sequence of Tournaisian taxa differed from those found with smaller values. In addition, slightly different branching patterns emerge for various early tetrapod taxa/groups following different implied weighting searches. Below, we highlight key differences among various tree topologies.

In trees generated with K = 3, 4 and 5, *Ossirarus*, *Perittodus* and *Diploradus* emerge as increasingly crownward taxa, in that sequence, along the tetrapod stem group, whilst *Aytonerpeton* and *Koilops* are placed among stem amphibians and are thus part of the tetrapod crown group. *Ossirarus* is crownward of a (*Ventastega* + *Ichthyostega*) clade, with *Ossinodus* placed either immediately anti-crownward of (K = 3), in a polytomy with (K = 4), or immediately crownward of *Ossirarus* (K = 5). *Perittodus* is the sister taxon to the Devonian *Ichthyostega*-like taxon *Ymeria*, and the (*Perittodus* + *Ymeria*) clade forms the sister group to *Pederpes*. *Diploradus* is immediately crownward of a (*Whatcheeria* + *Occidens*) clade, which in turn occurs crownward of (*Pederpes* + (*Perittodus* + *Ymeria*)). However, the branching sequence of Carboniferous stem

754 tetrapods more crownward than *Diploradus* varies. Thus, in trees with K = 3, the
755 branching sequence includes *Crassigyrinus*, *Doragnathus*, (*Megalocephalus* +
756 *Baphetes*) and *Loxomma*. In trees with K = 4, the sequence includes only *Crassigyrinus*
757 and *Doragnathus*, whereas all baphetids form a clade on the amphibian stem
758 (*Megalocephalus* + (*Loxomma* + *Baphetes*)). In trees with K = 5, the baphetid clade is,
759 once again, on the amphibian stem, but the sequence of stem tetrapods crownward of
760 *Diploradus* differs substantially, and includes (*Eucritta* + *Doragnathus*), *Sigournea* and
761 *Crassigyrinus*. In trees from K = 3 and 4, the (*Aytonerpeton* + *Sigournea*) clade forms
762 the sister group to a (*Koilops* + (*Tulerpeton* + (*Greererpeton* + *Colosteus*))) clade. In
763 turn, this wider group joins temnospondyls on the amphibian stem, with *Caerorhachis* as
764 a more immediate sister taxon. In trees from K = 5, *Aytonerpeton* is collapsed in a
765 trichotomy with temnospondyls and the (*Koilops* + (*Tulerpeton* + (*Greererpeton* +
766 *Colosteus*))) clade. With K = 10, the results match those from the second set of
767 parsimony analyses (reweighting).
768 As for other tetrapod groups, the amniote stem undergoes little reshuffling in
769 trees derived from different K values. The most noticeable difference among such trees
770 is the placement of *Silvanerpeton* and *Gephyrostegus*, both of which are immediately
771 crownward of the 'anthracosauroids' (*Eoherpeton* + (*Pholiderpeton* + *Proterogyrinus*))
772 but swap their positions as the first and second most crownward plesion after
773 anthracosauroids.
774 With characters reweighted by the maximum value of the rescaled consistency
775 index, we found three trees differing only in the relative positions of *Whatcheeria*,
776 *Pederpes* and *Occidens*, all of which form a clade. In those trees, all new Tournaisian
777 taxa appear on the tetrapod stem. In particular, *Aytonerpeton* and *Perittodus* are sister
778 taxa, and together they join *Ymeria*. In crownward order, the sequence of stem tetrapods

includes: *Acanthostega*, *Ossinodus*, *Ventastega*, *Ichthyostega*, *Ossirarus*, the (*Ymeria* (*Aytonerpeton* + *Perittodus*)) clade, the (*Whatcheeria*, *Pederpes*, *Occidens*) clade, *Diploradus*, *Doragnathus*, *Sigournea*, a (*Koilops* + (*Tulerpeton* + (*Greererpeton* + *Colosteus*))) clade, *Crassigyrinus*, and a baphetid clade. *Caerorhachis* and *Eucritta* appear as the earliest diverging plesions on the amphibian and amniote stem groups, respectively.

Sedimentological and Environmental Interpretation

The borehole was located at Norham near Berwick-Upon-Tweed (British National Grid Reference [BNGR] 391589, 648135), and the Burnmouth section is at BNGR 396000-661000.

The stratigraphical position of the succession at Willie's Hole is inferred from a nearby borehole (Hutton Hall Barns, BGS Registered number NT85SE1. The exact stratigraphical position of the Willie's Hole (WH) section is uncertain within the overall succession. No direct correlation with the succession recorded in the Hutton Hall Barns borehole is possible because the borehole is an old one and the level of detail insufficient, plus the fact that distinctive markers are not present in the Ballagan Formation. However, that borehole proved 142.5m of Ballagan Formation strata - the log is good enough to define precisely where the base is, resting on Kinnesswood Formation. The proximity of WH to the borehole allows us to infer that the WH section lies approximately 150m above the base of the Ballagan Formation. The palynological samples from WH contained *Umbonatisporites distinctus*, a spore that is only found in the lower part of our borehole core. We argue that therefore the WH section belongs to the lower part of the Ballagan Formation. We indicated some uncertainty in the figure and gave an approximate range.

The dominance of actinopterygians and rhizodonts within these lakes indicates brackish-freshwater salinity levels [50,51]. Diverse palaeosols[15] and palynology suggest habitats including forest, low-growing and creeping flora, wetland and desiccating pools traversed by rivers (predominantly meandering channels) and saline-hypersaline lakes depositing cementstones and evaporites (Fig. 6 **and Supplementary Fig. 7**)[27-31,52] The saline-hypersaline lake deposits in the Ballagan Formation have been interpreted to represent brackish marginal marine or hypersaline[52-56] conditions. Other dolomitic units from the Mississippian are interpreted as saline coastal marshes[56-61]. Erosive-based, cross-bedded sandstone units (one to tens of metres thick) with basal conglomerate lags cut into all other facies[34]. The lags contain disarticulated vertebrate material including acanthodian, rhizodont and tetrapod bones[16].

Charcoal Analysis

Dispersed organic matter (DOM) was extracted by standard palynological demineralisation techniques[62]. Measurement of maceral reflectance in oil was by means of a Zeiss UMSP 50 Microspectrophotometer, housed in the School of Ocean and Earth Science, National Oceanography Centre Southampton, University of Southampton Waterfront Campus. Measurements were made under standard conditions as defined by the International Committee for Coal Petrology[63].

Model-based estimates of atmospheric oxygen concentration during the early Tournaisian vary from 10 – 20%, with more recent models favouring the higher figure[64-68]. As an alternative, fossil charcoal (fusinite) is used by several authors as a

826 proxy for atmospheric oxygen[69-72], as wildfire activity, and hence charcoal production,
827 is proportional to oxygen supply [73]. Controlled burning experiments [73] have
828 demonstrated that when O_2 exceeds the present atmospheric level (PAL) of 20.9%, fire
829 activity rapidly increases and reaches a plateau at around 24%; therefore, we infer that
830 fusinite abundance is likely insensitive to any further increase. Conversely, fire activity
831 is strongly supressed below 20% O_2 and switched off completely below 16%, even in
832 very dry conditions[73].The most comprehensive attempt thus far to reconstruct
833 Phanerozoic O_2 in this way[69] indicated 25.6% O_2 during Romer's Gap – substantially
834 higher than PAL and exceeding the presumed upper limit of fusain sensitivity (24%).
835 However, this study was based on the inertinite (= microscopic fusinite) content of
836 coals, which are infrequent during the Tournaisian, so sampling density was relatively
837 low. Furthermore, we assume that large-scale forest fires will have a far greater
838 influence on coal deposits, formed in situ in forest mires, than on the more distal
839 deposits of the kind examined here.
840 By focusing on DOM extracted from sedimentary rocks other than coal, fusinite
841 content can be measured through stratigraphic successions in which coals are rare or
842 absent. The values reported here represent the proportion of fusinite within the organic
843 matter isolated from each 5g shale sample, based on examination of 500 organic (i.e.
844 plant derived) macerals. This indicates the proportion of plant-derived material in the
845 sample which has been burned at high temperatures, and is therefore independent of
846 sediment supply.
847 The specific Famennian and Viséan sampling localities chosen were selected because, as
848 well as being of the required age:
849 • The stratigraphic context of the sampled formations is well understood, with

well-established biozonation (**Supplementary Table 1**).

- Thermal maturity in these successions is low. This is essential, because with increasing thermal maturity the reflectance of non-pyrolitic macerals (most notably vitrinite) increases, eventually rendering them indistinguishable from fusinite.
- Both localities represent largely terrestrial environments, containing a succession of fluviodeltaic, lacustrine or nearshore marine deposits (**Supplementary Table 1**). Sediments deposited in such environments represent an accumulation point for river-transported organic material derived from the wider region; this mitigates the distorting effect of local fire activity,

The organic maceral fusinite is considered synonymous with charcoal and can be distinguished from other maceral types by its reflectance under incident light[74]; we have focused solely on fusinite for this study because, although most other members (semi-fusinite) of the inertinite group are also accepted as pyrolitic in origin[75], their reflectance forms a continuum between that of vitrinite and fusinite and forms the bulk of the organic matter. This makes the % sum of semi-fusinite and fusinite very large (>90%) and less reliable.

Supplementary Data Table 1b gives the samples taken from Famennian sites, Burnmouth, Willie's Hole and Visean sites. These were analysed for charcoal content. Mean abundance was 2.0%, which is within error of data obtained from Burnmouth Shore, suggesting that the contribution from local fire activity (if any) was similar at both sites (**Supplementary Table 1 and Supplementary Fig. 9**).

Data availabiltity statement. Correspondence and requests for materials should be addressed to Jennifer A. Clack j.a.clack@zoo.cam.ac.uk. Specimen information is

available from the respective housing institutions. Micro-CT scan data to be placed in the NERC National Geoscience Data Centre.

Author contributions

JAC is corresponding author and lead PI and with TRS, JAC, BKAO, and KZS collected, described and analysed the tetrapod specimens. CEB, TIK, SJD and DM contributed to the stratigraphical, sedimentological and environmental studies. JEAM, DKC, and EJR contributed to the charcoal, palynological and stratigraphical studies. MR and JAC contributed to the phylogenetic analysis. AJR contributed information on the arthropods, SAW provided additional work on micro-CT scan data. AJR, SAW and NCF organised the Willie's Hole excavation that provided sedimentological information. All authors contributed to discussion, preparation and writing the paper.

Acknowledgements

We acknowledge funding from NERC consortium grants NE/J022713/1 (Cambridge), NE/J020729/1 (Leicester), NE/J021067/1 (BGS), NE/J020621/1 (NMS), NE/J021091/1 (Southampton). We thank the following for their support and contributions. Stan and Maggie Wood for discovery of and access to collections, Oliver and Betty Kieran and Burnmouth community for support for the project, Mike Browne for field assistance and information on stratigraphy, Matt Lowe for access to UMZC collections, Sarah Finney for field assistance, conservation advice and preparation of *Koilops*, Vicen Carrió for conservation and preparation of NMS specimens, Janet Sherwin for stratigraphy and field assistance. Shir Akbari (Southampton) contributed to palynological processing. TIK and DM publish with the permission of the Executive Director, British Geological Survey (NERC). Anne Brown and Colin MacFadyen of Scottish Natural Heritage gave

permission to collect at sites in their care, and Paul Bancks from The Crown Estates Office in Edinburgh, gave permission to collect on Crown land. PRISM, the Isaac Newton Trust Fund (Trinity College, Cambridge), the Crotch Fund (UMZC) and an anonymous donor provided funding for purchase of specimens. This is a contribution to IGCP project 596.

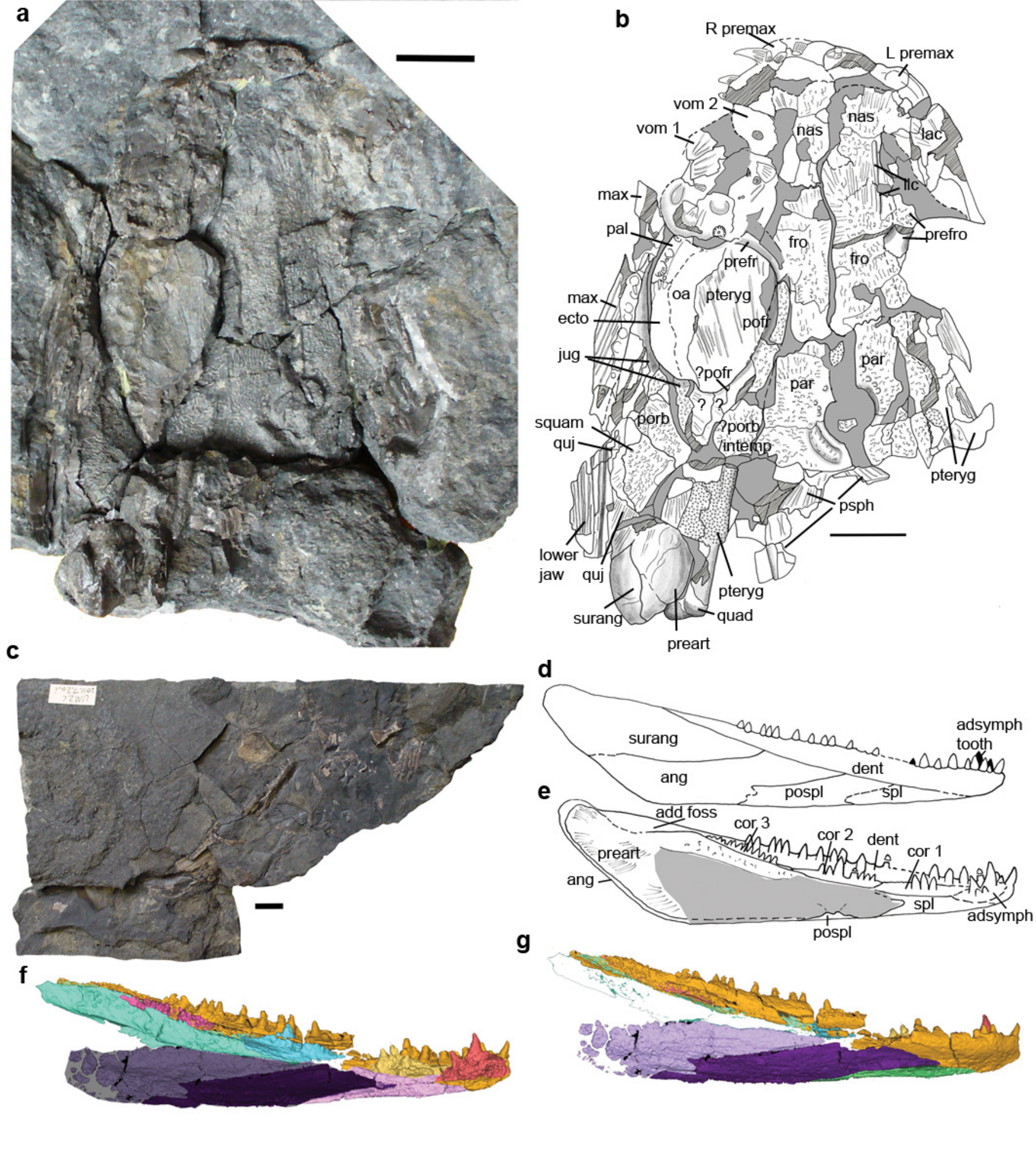
a
b
R premax
L premax
vom 2
vom 1
nas
nas
lac
llc
max
pal
prefro
fro
fro
prefr
max
oa
pteryg
ecto
pofr
jug
?pofr
par
par
? ?
squam
porb
?porb
quj
interp
pteryg
psph
lower
jaw
quj
pteryg
surang
quad
preart
c
d
adsymph
tooth
surang
dent
ang
pospl
spl
e
add foss
cor 3
cor 2
dent
cor 1
preart
ang
spl
adsymph
pospl
g
f

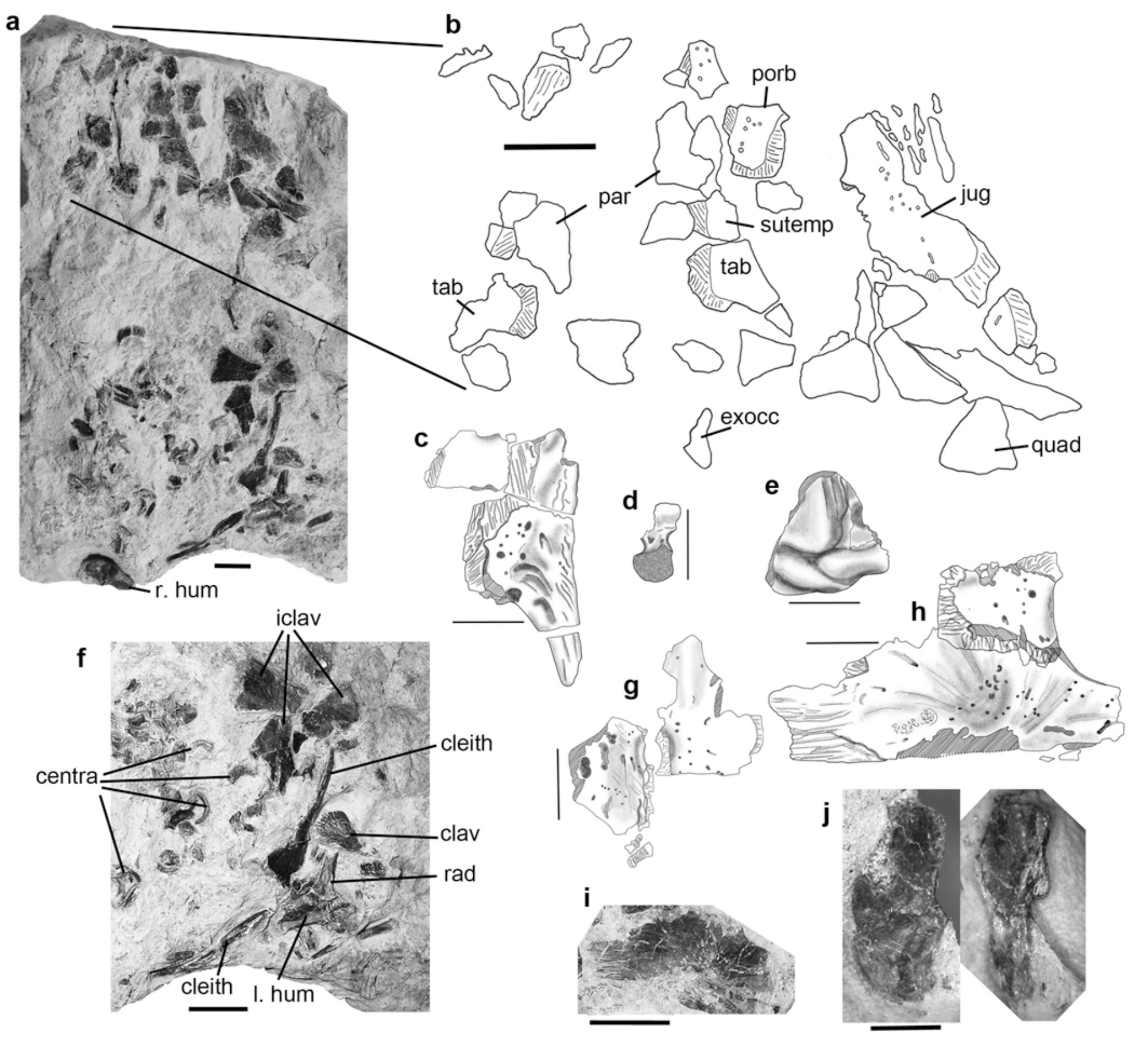
a
b
porb
par
jug
sutemp
tab
tab
exocc
quad
r. hum
c
d
e
h
g
f
iclav
cleith
centra
clav
rad
cleith
l. hum
i
j

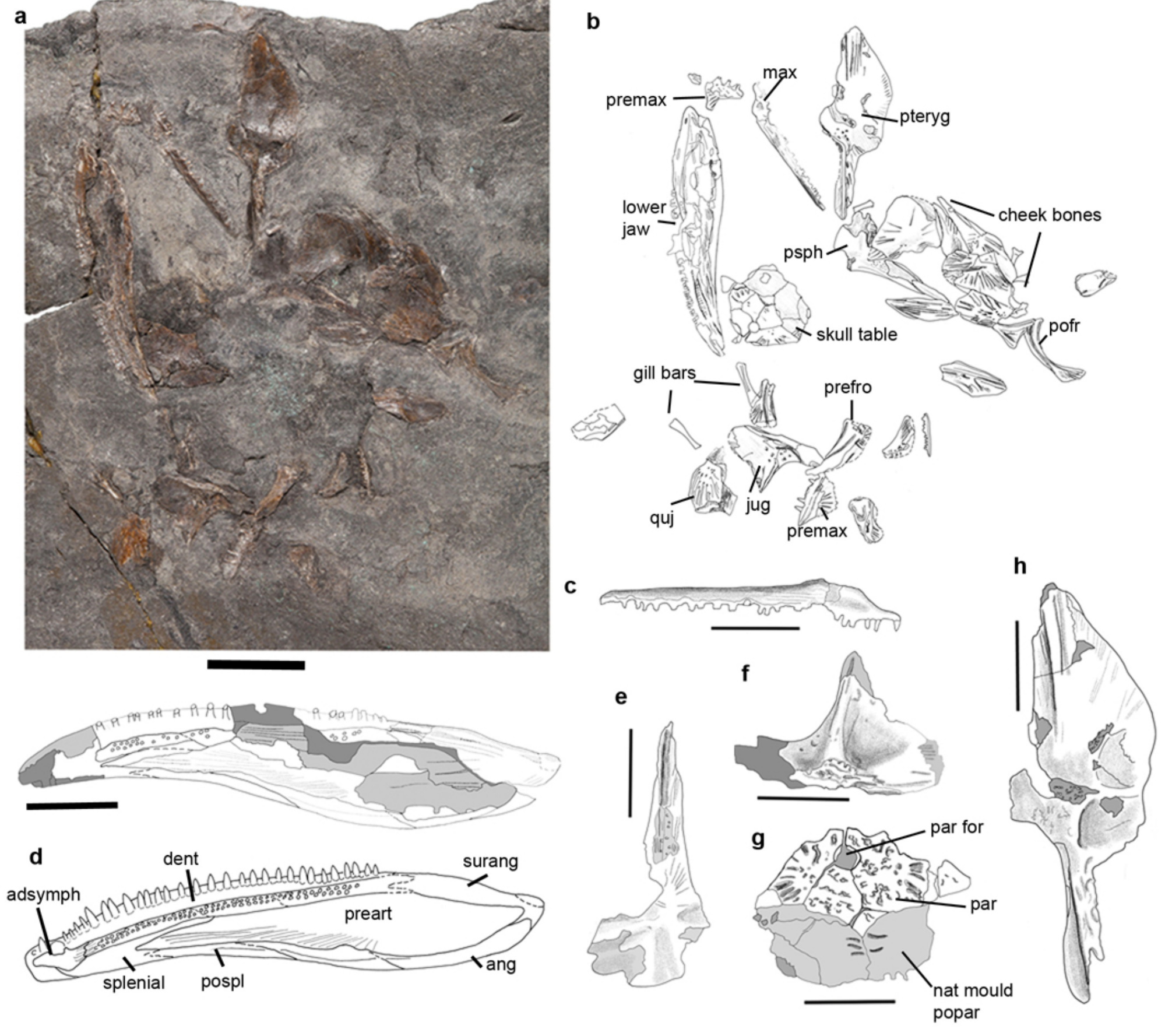
a
b
premax
max
pteryg
lower jaw
cheek bones
psph
skull table
pofr
gill bars
prefro
quj
jug
premax
c
h
e
f
g
par for
par
nat mould popar
d
dent
surang
adsymph
preart
splenial
pospl
ang

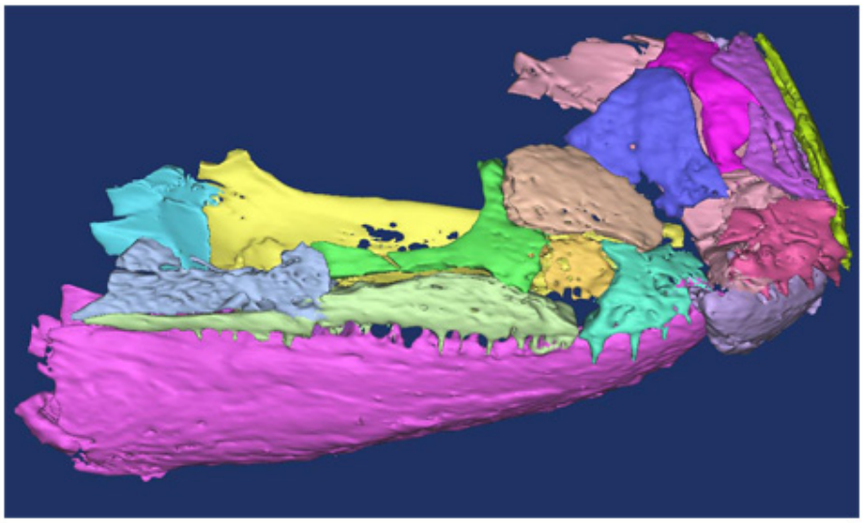

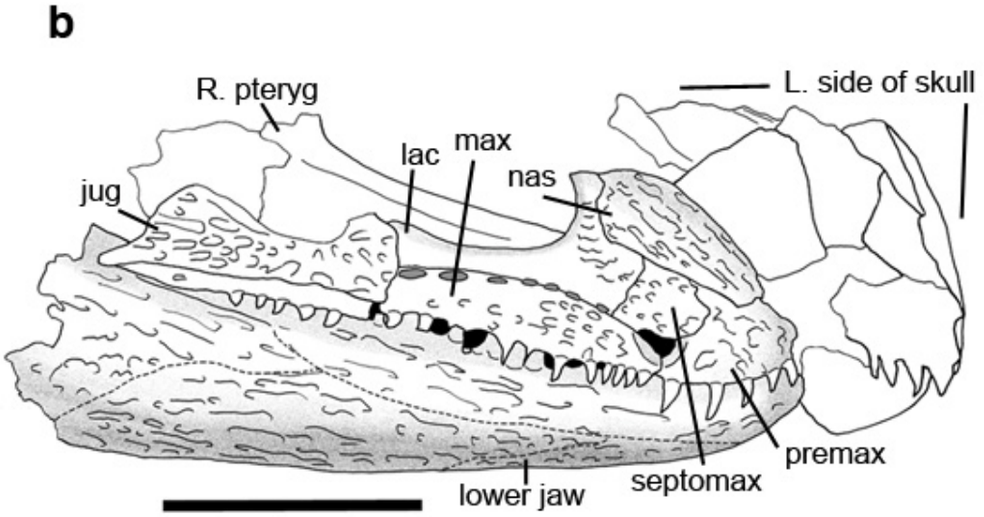
b
R. pteryg
L. side of skull
lac
max
nas
jug
premax
septomax
lower jaw

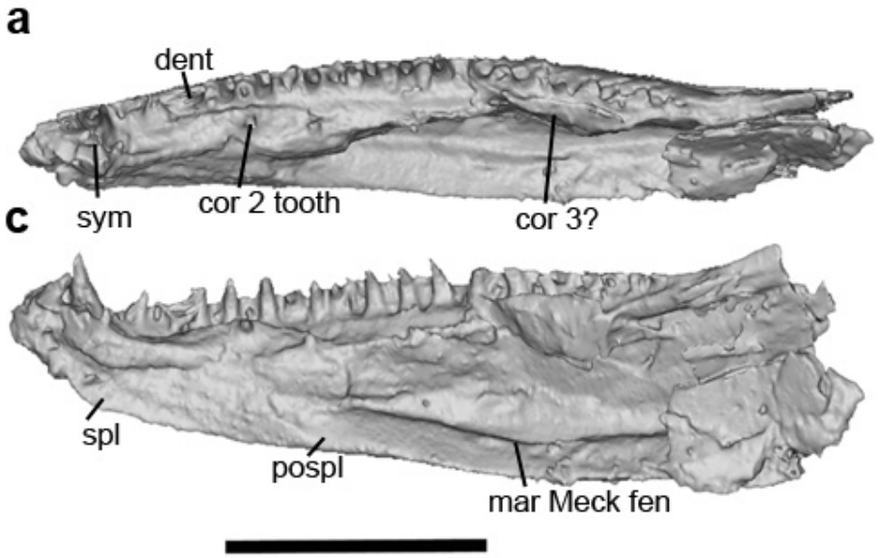
a
dent
sym
cor 2 tooth
cor 3?
c
spl
pospl
mar Meck fen

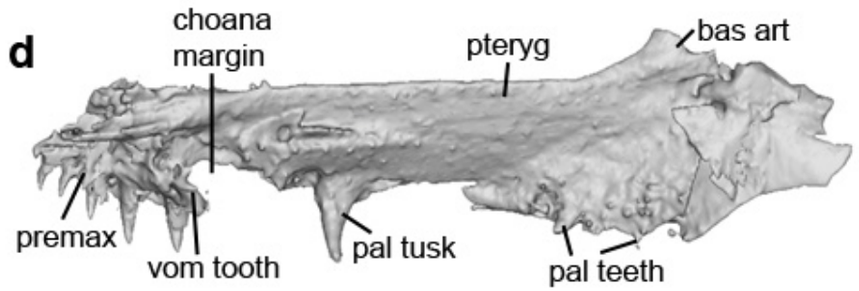
d
choana margin
pteryg
bas art
premax
vom tooth
pal tusk
pal teeth

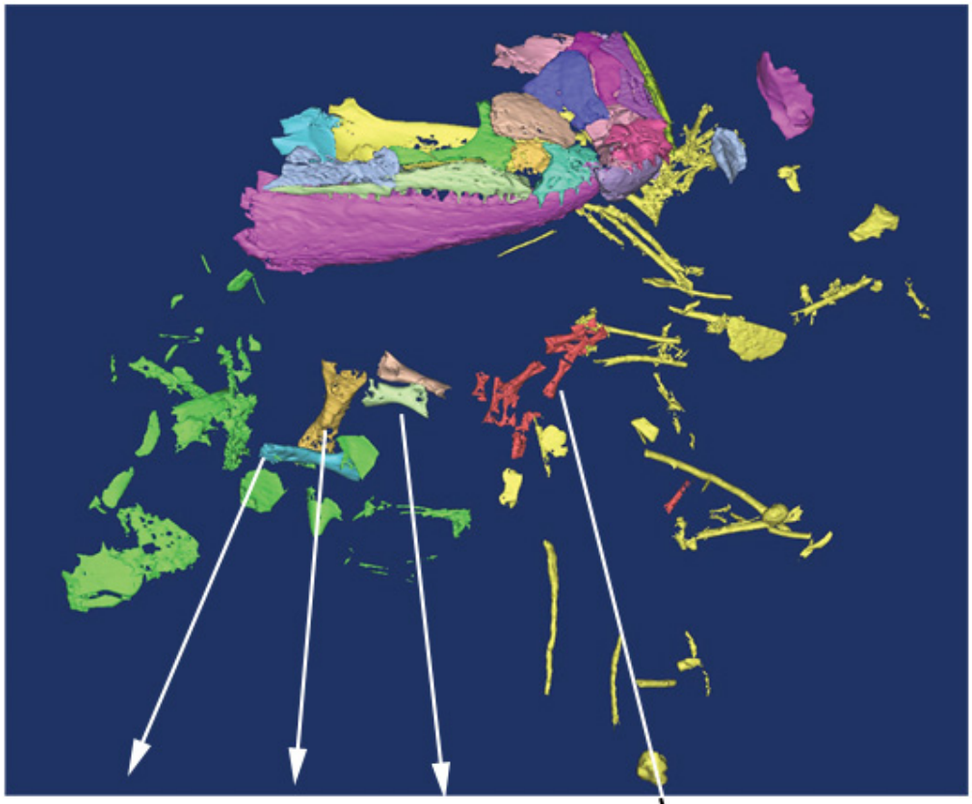

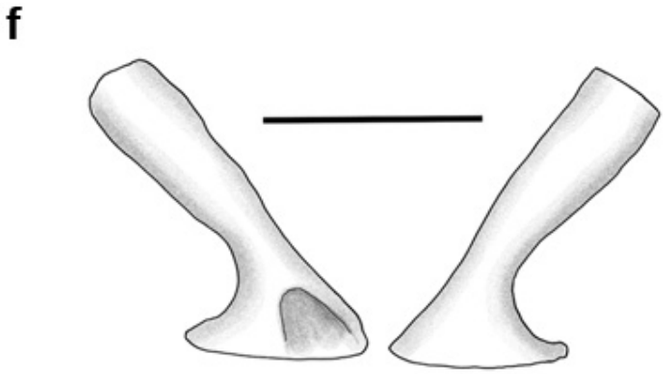
f

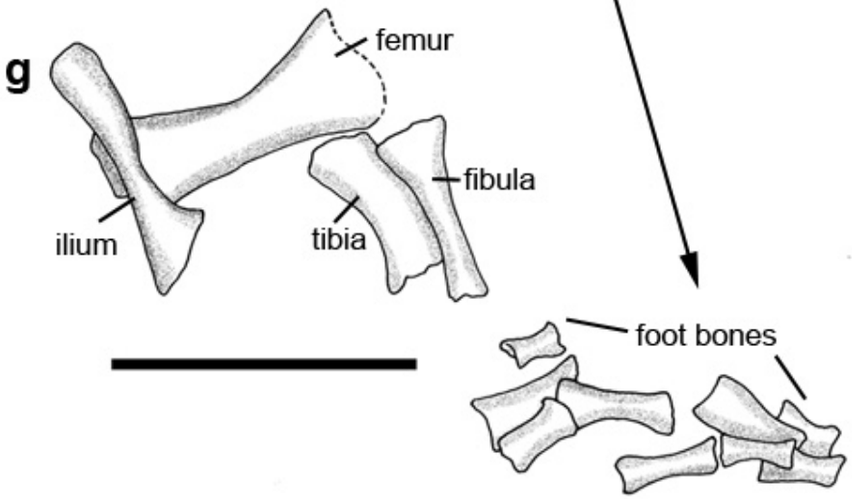
g
femur
fibula
ilium
tibia
foot bones

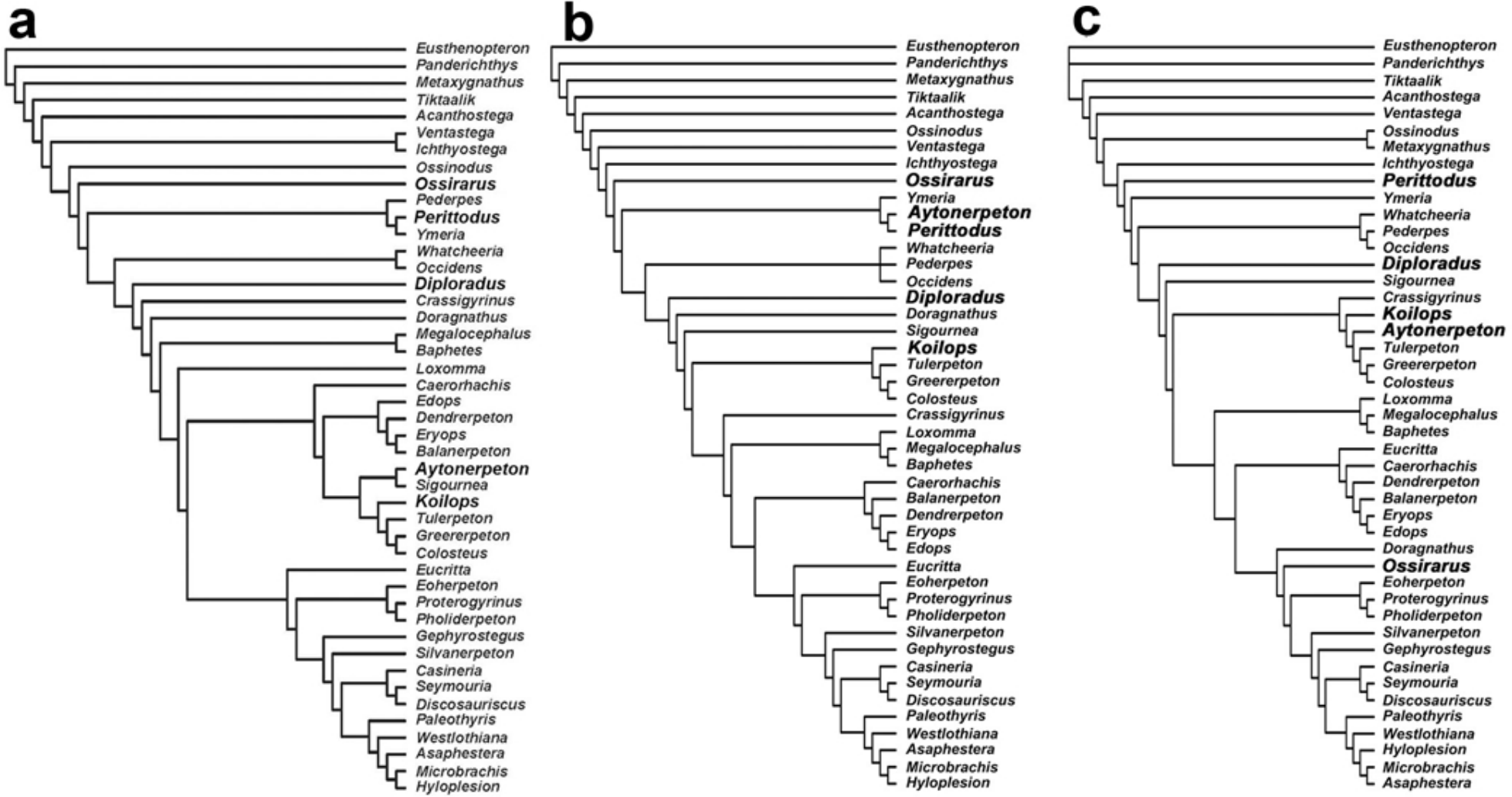
a
Eusthenopteron
Panderichthys
Metaxygnathus
Tiktaalik
Acanthostega
Ventastega
Ichthyostega
Ossinodus
Ossirarus
Pederpes
Perittodus
Ymeria
Whatcheeria
Occidens
Diploradus
Crassigyrinus
Doragnathus
Megalocephalus
Baphetes
Loxomma
Caerorhachis
Edops
Dendrerpeton
Eryops
Balanerpeton
Aytonerpeton
Sigournea
Koilops
Tulerpeton
Greererpeton
Colosteus
Eucritta
Eoherpeton
Proterogyrinus
Pholiderpeton
Gephyrostegus
Silvanerpeton
Casineria
Seymouria
Discosauriscus
Paleothyris
Westlothiana
Asaphestera
Microbrachis
Hyloplesion
b
Eusthenopteron
Panderichthys
Metaxygnathus
Tiktaalik
Acanthostega
Ossinodus
Ventastega
Ichthyostega
Ossirarus
Ymeria
Aytonerpeton
Perittodus
Whatcheeria
Pederpes
Occidens
Diploradus
Doragnathus
Sigournea
Koilops
Tulerpeton
Greererpeton
Colosteus
Crassigyrinus
Loxomma
Megalocephalus
Baphetes
Caerorhachis
Balanerpeton
Dendrerpeton
Eryops
Edops
Eucritta
Eoherpeton
Proterogyrinus
Pholiderpeton
Silvanerpeton
Gephyrostegus
Casineria
Seymouria
Discosauriscus
Paleothyris
Westlothiana
Asaphestera
Microbrachis
Hyloplesion
c
Eusthenopteron
Panderichthys
Tiktaalik
Acanthostega
Ventastega
Ossinodus
Metaxygnathus
Ichthyostega
Perittodus
Ymeria
Whatcheeria
Pederpes
Occidens
Diploradus
Sigournea
Crassigyrinus
Koilops
Aytonerpeton
Tulerpeton
Greererpeton
Colosteus
Loxomma
Megalocephalus
Baphetes
Eucritta
Caerorhachis
Dendrerpeton
Balanerpeton
Eryops
Edops
Doragnathus
Ossirarus
Eoherpeton
Proterogyrinus
Pholiderpeton
Silvanerpeton
Gephyrostegus
Casineria
Seymouria
Discosauriscus
Paleothyris
Westlothiana
Hyloplesion
Microbrachis
Asaphestera

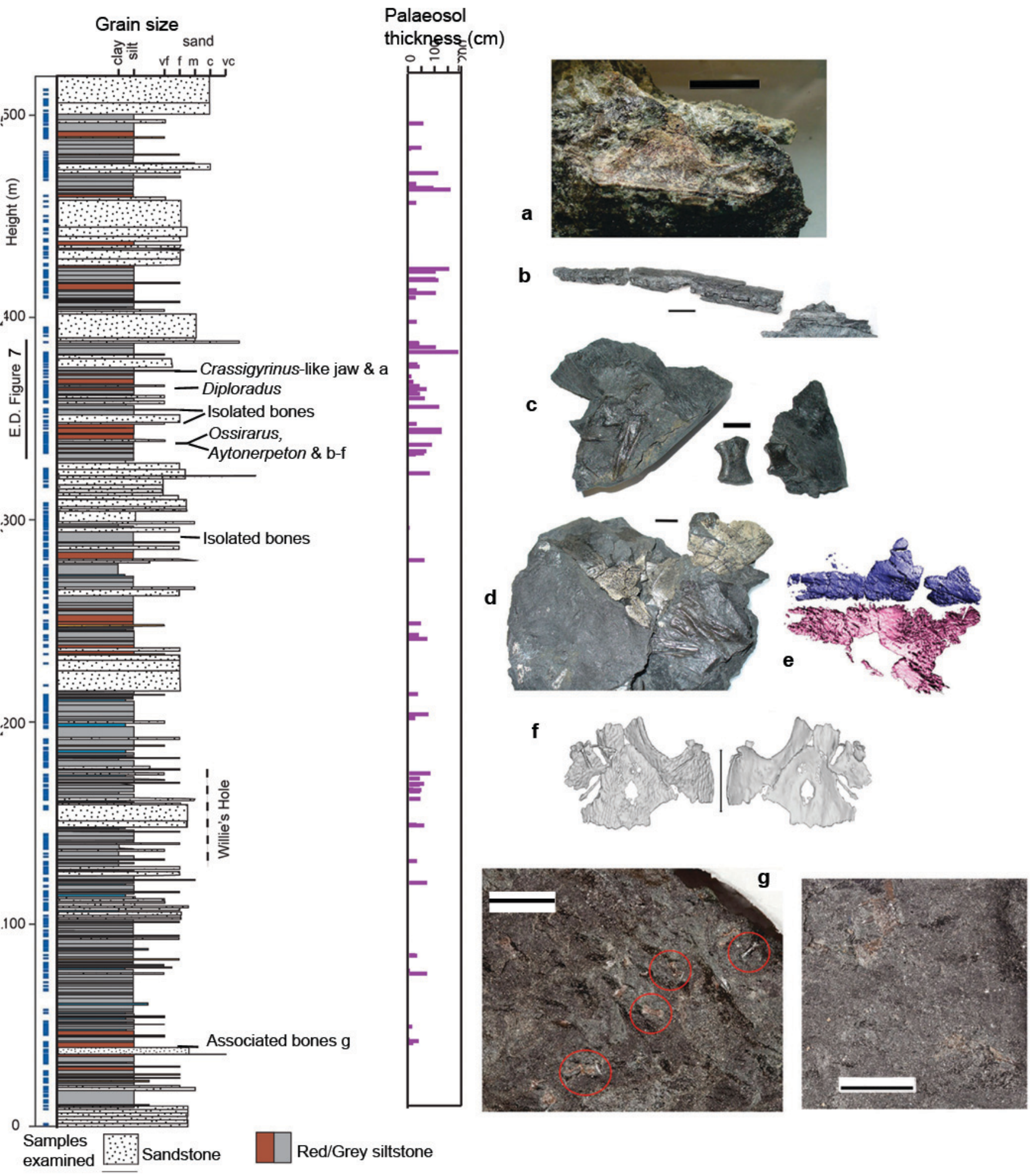
Grain size
clay
silt
sand
vf f m c vc
Palaeosol thickness (cm)
0
100
200
Height (m)
500
400
300
200
100
0
E.D. Figure 7
Crassigyrinus-like jaw & a
Diploradus
Isolated bones
Ossirarus,
Aytonerpeton & b-f
Isolated bones
Willie's Hole
Associated bones g
Samples examined
Sandstone
Red/Grey siltstone
a
b
c
d
e
f
g

Phylogenetic and Environmental Context of a Tournaisian Tetrapod Fauna

Clack et al.

Supplementary Information contains

S**upplementary Video file 1 (.mov)**. This shows the skull of *Aytonerpeton* as a rotational view of the 3-D skull in the main text Figure 4. (12.7 MB)

Supplementary Video file 2 (.mov). This shows the whole block containing *Aytonerpeton* including the skull and postcranial elements as a rotational view in 3-D.

Supplementary Figures

Fig. 1. Locality map.

Figs 2-6. Figures of additional tetrapod specimens. The tetrapod fossils in this collection represent conservatively a sample of at least 7 new taxa, but possibly more. A further taxon is represented by NMS G.2012.39.22 ("Ribbo" in ref 2). The *Crassigyrinus*-like jaw UMZC 2011.9.1 in ref 2 may belong to one of those figured here, or to NMS G.2012.39.22, although the dermal ornamentation does not match that in any of them.

Fig. 7. Detailed log of the most productive section of the Burnmouth sequence, and the changing palaeoenvironment that it represents.

Fig. 8. Three additional cladograms.

Fig. 9. Box plot of fusinite abundances from the Famennian – Visean.

Supplementary Data. This contains a pdf of the character list with the sources for the characters and the data matrix used in the cladistic analysis.

Supplementary Table shows fusinite sampling sites, numbers of samples and environments, and fusinite abundances from the Famennian, Tournaisian and Visean.

Phylogenetic and Environmental Context of a Tournaisian Tetrapod Fauna

Clack et al.

Supplementary Information contains

S**upplementary Video file 1 (.mov)**. This shows the skull of *Aytonerpeton* as a rotational view of the 3-D skull in the main text Figure 4. (12.7 MB)

Supplementary Video file 2 (.mov). This shows the whole block containing *Aytonerpeton* including the skull and postcranial elements as a rotational view in 3-D.

Supplementary Figures

Fig. 1. Locality map.

Figs 2-6. Figures of additional tetrapod specimens. The tetrapod fossils in this collection represent conservatively a sample of at least 7 new taxa, but possibly more. A further taxon is represented by NMS G.2012.39.22 ("Ribbo" in ref 2). The *Crassigyrinus*-like jaw UMZC 2011.9.1 in ref 2 may belong to one of those figured here, or to NMS G.2012.39.22, although the dermal ornamentation does not match that in any of them.

Fig. 7. Detailed log of the most productive section of the Burnmouth sequence, and the changing palaeoenvironment that it represents.

Fig. 8. Three additional cladograms.

Fig. 9. Box plot of fusinite abundances from the Famennian – Visean.

Supplementary Data. This contains a pdf of the character list with the sources for the characters and the data matrix used in the cladistic analysis.

Supplementary Table shows fusinite sampling sites, numbers of samples and environments, and fusinite abundances from the Famennian, Tournaisian and Visean.

Phylogenetic and Environmental Context of a Tournaisian Tetrapod Fauna

Clack et al.

Supplementary Information

Supplementary Figures

Figure 1. A locality map of the fossil-bearing sites.

Figures 2-6. The tetrapod fossils in this collection represent conservatively a sample of at least 7 new taxa, but possibly more. A further taxon is represented by NMS G.2012.39.22 ("Ribbo" in ref 2). The *Crassigyrinus*-like jaw UMZC 2011.9.1 in ref 2 may belong to one of those figured here, or to NMS G.2012.39.22, although the dermal ornamentation does not match that in any of them.

Figure 7. Detailed log of the most productive section of the Burnmouth sequence, and the changing palaeoenvironment that it represents.

Figure 8. Three additional cladograms.

Figure 9. Box plot of fusinite abundances from the Famennian – Visean.

Supplementary Data. Character list with the sources for the characters and the data matrix used in the cladistic analysis.

Supplementary Table Fusinite sampling sites, numbers of samples and environments, and fusinite abundances from the Famennian, Tournaisian and Visean.

Supplementary Figure 1: Map showing distribution of tetrapod-bearing localities in Scotland. Inset – Borders Region on the east coast where most of the finds have been made.

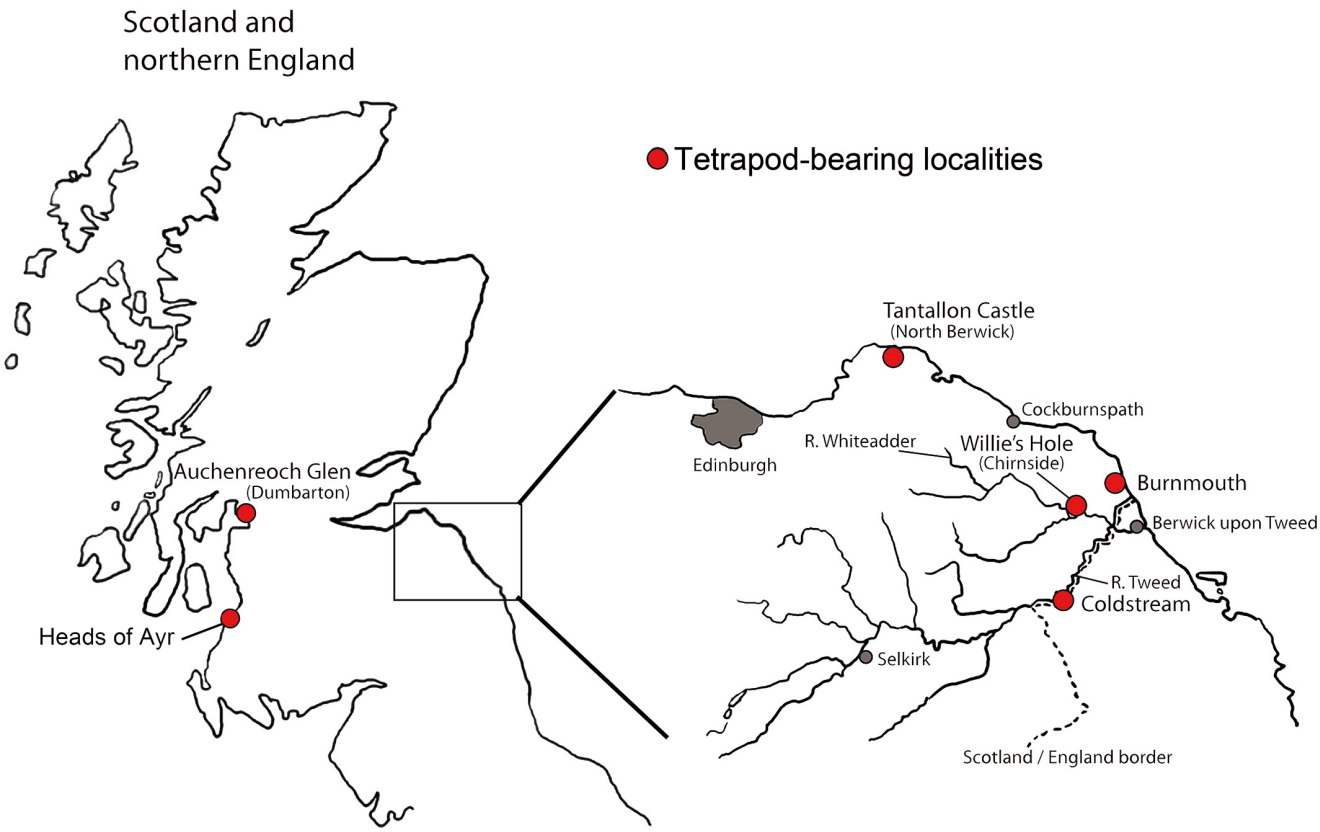

Supplementary Figure 2: Associated skull and other bones (UMZC 2016. 6 a-d) from the same Burnmouth horizon yielding *Aytonerpeton microps* (main text Fig.4). Probable new taxon 2.

a, Micro-CT scan of bones including a parasphenoid in ventral view, a dentary or maxilla, a jugal, a probable postorbital, a possible clavicle, centrum and ribs. **b**, The parasphenoid in dorsal view showing the dorsum sellae. **c**, Photograph of the external surface of the block with a close-up of the parasphenoid and jaw elements. The dentition and jugal bones are unlike those of *Aytonerpeton*, and the parasphenoid is unlike those of either colosteids or temnospondyls from later in the Carboniferous. The short dorsum sellae is similar to that of some later temnospondyls, but the extent of the denticulation on the posterior plate of the parasphenoid is unique. (Photograph by T. R. Smithson, micro-CT by K. Z. Smithson

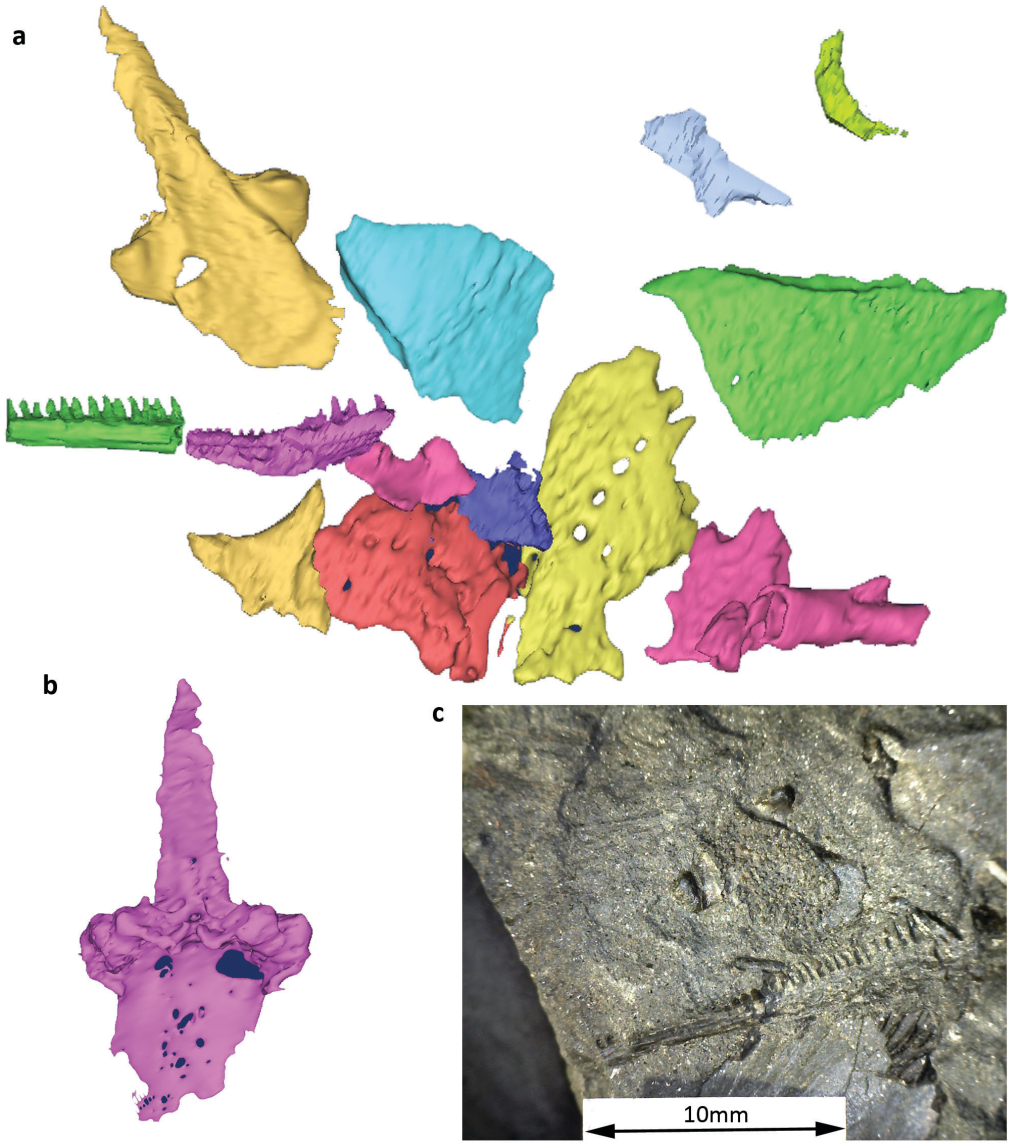

Supplementary Figure 3: Two skulls representing new taxa from Willie's Hole (SPW bed 2).
a, A small skull (NMS G. 2012.39.77) in part and counterpart. Probable new taxon 3.The skull is highly fractured, each part and counterpart showing both palatal and skull roofing bones. The position of the orbits cannot be ascertained. The drawing in **b**, is based on information from both part and counterpart. Notable is the evidence for a closed palate in a skull with a strongly embayed squamosal for a spiracular or possibly otic notch, a unique combination of features in a Tournaisian tetrapod. There is almost no overlap in the preserved bones with those of *Ossirarus*, but it is clear that it does not share the distinctive tabular with that taxon, and its dermal ornament is quite different. Although NMS G. 2012.39.77 is smaller than *Ossirarus*, it is equally well ossified. 10 mm scale bar on photographs. (Photographs by T. R. Smithson); **c,** Part of a skull roof in natural mould, from Willie's Hole (NMS G. 2012.39.95). Probable new taxon 4. The specimen has associated skull bones, phalanges and an ilium. The shape of the parietal foramen, the impression left by its surrounding bones, and its proportions distinguish it from *Koilops herma*. Scale bar 10 mm. (Photograph by J. A. Clack)

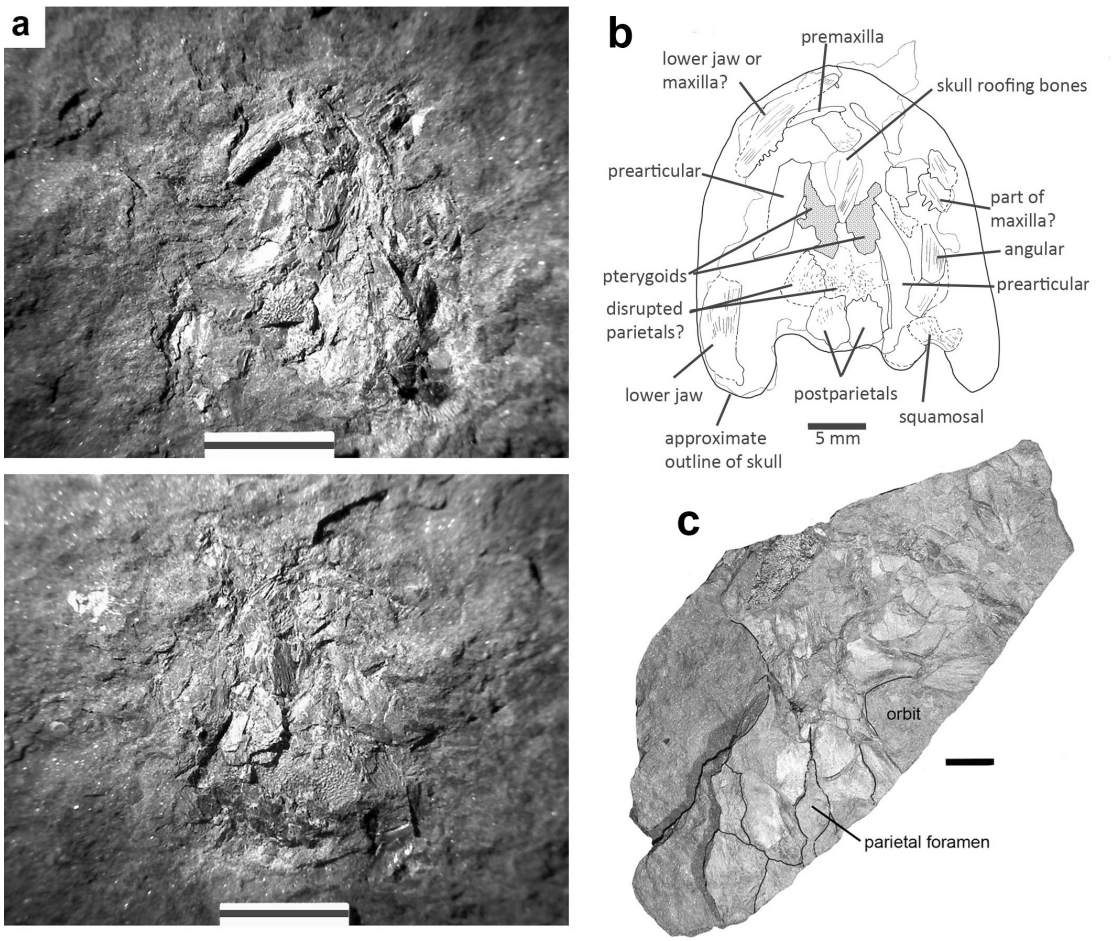

Supplementary Figure 4: UMZC 2011.7.16, a large tetrapod in part and counterpart from Willie's Hole (SPW bed 2). Probable new taxon 5. The specimen includes an interclavicle similar to that of *Pederpes*, and fragments of the skull, numerous ribs and belly scales, a few centra, and epipodials, none of which resembles those of *Pederpes*. The ribs do not bear flanges, the centra are less well ossified, and the epipodials are much more slender. There are also rectangular and lightly ornamented probable dorsal scales (inset, arrows. Inset also shows belly scales). This specimen does not resemble that of NMS G. 2012.39.22 ("Ribbo" in ref 2) in which the ribs are longer and more curved. Scale bar in inset, 10 mm. (Photographs by J. A. Clack and T. R. Smithson)

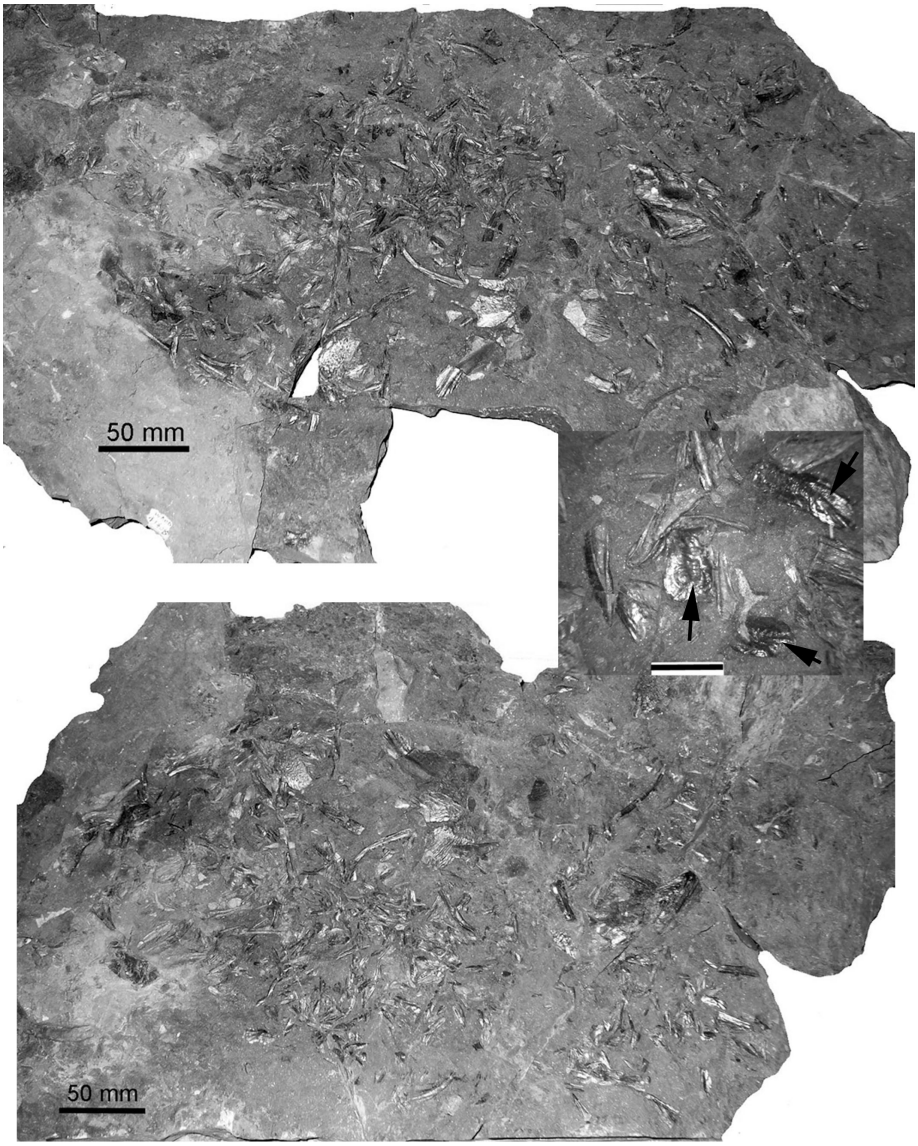

Supplementary Figure 5: UMZC 2011.7.13, a large jaw and scattered skull bones from Willie's Hole (SPW bed 2). Probable new taxon 5?
a, Isolated skull bones collected from the specimen by S. P. Wood include a tabular that is similar to that of *Crassigyrinus*, although there are no other obvious similarities between the two. **b,** Whole specimen. **c**, Belly scales, similar to those in UMZC 2011. 7.16. **d**, Teeth show a recurved tip and lateral keels that are not found in other tetrapods from the Tournaisian collection. However, there are no teeth preserved in UMZC 2011. 7.16, so that attribution of these two specimens to the same taxon cannot be ruled out. Scale bars in **a-c** are 10 mm, in **d**, 5 mm. (Photographs by J. A. Clack and T. R. Smithson)

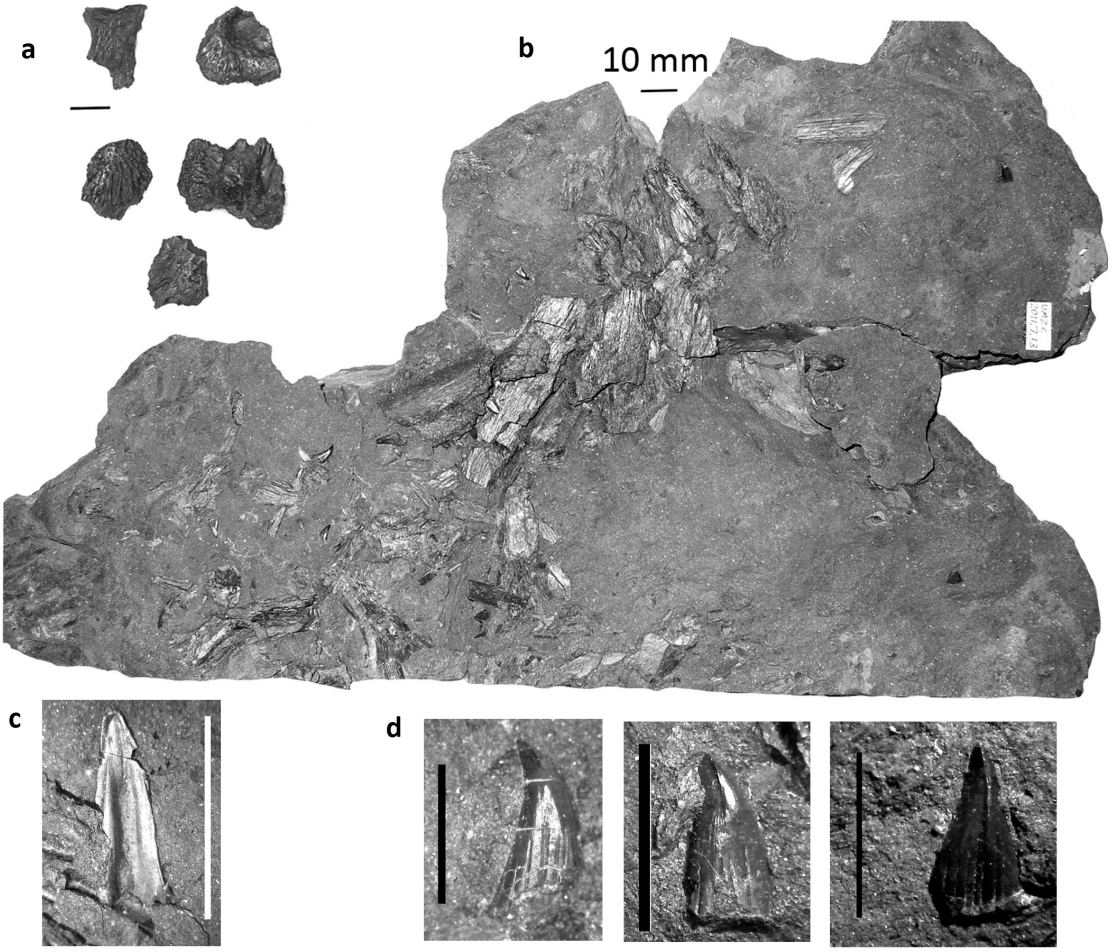

Supplementary Figure 6. a,b, A small humerus from Tantallon Castle, Gin Head (NMS G.2016.15.1). Probable new taxon 7. **c,** A maxilla in part and counterpart from the Heads of Ayr.
a, views left to right: ventral; posteroventral; anterior. **b,** from a micro-CT scan, views left to right: dorsal, ventral, posterior, anterior. Note the large deltopectoral process (dpc), placed anterior to a recognizable shaft, and the extent of torsion between proximal and distal ends. The conspicuous latissimus dorsi process (ldp) is shared with *Baphetes* and *Pederpes*, but the overall shape of the humerus is quite different from those two. The matrix is a crudely bedded coarse volcaniclastic sedimentary rock, containing ostracods, bivalves and fish remains. **c,** Maxilla from Heads of Ayr, possibly similar to that in main text Fig. 6. Scale bars 10 mm (Photographs by T. R. Smithson, micro-CT images by K. Z. Smithson)

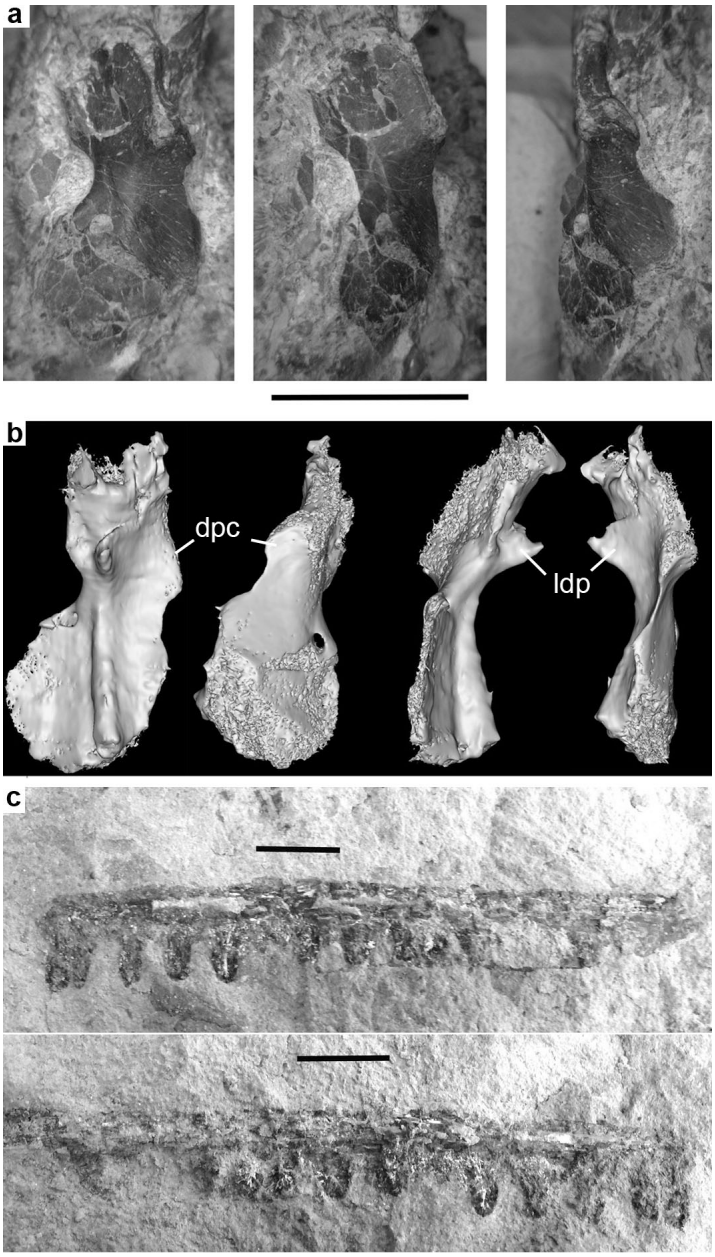

Supplementary Figure 7: Sedimentary conditions associated with the tetrapods. Palaeoenvironment of two of the tetrapod deposits. Left: Sedimentary log of partial section at Burnmouth with *Aytonerpeton* and *Ossirarus*, from 332 to 356 metres above the base of the Ballagan Formation. Between the sandstone units at the top and base of this section the sedimentary rocks comprise an overbank facies association. This succession records the transition from wet to dry conditions through time, with environments illustrated in the reconstructions for dry and wet periods (right). The tetrapod fossil-bearing horizons within this section are sandy siltstones.

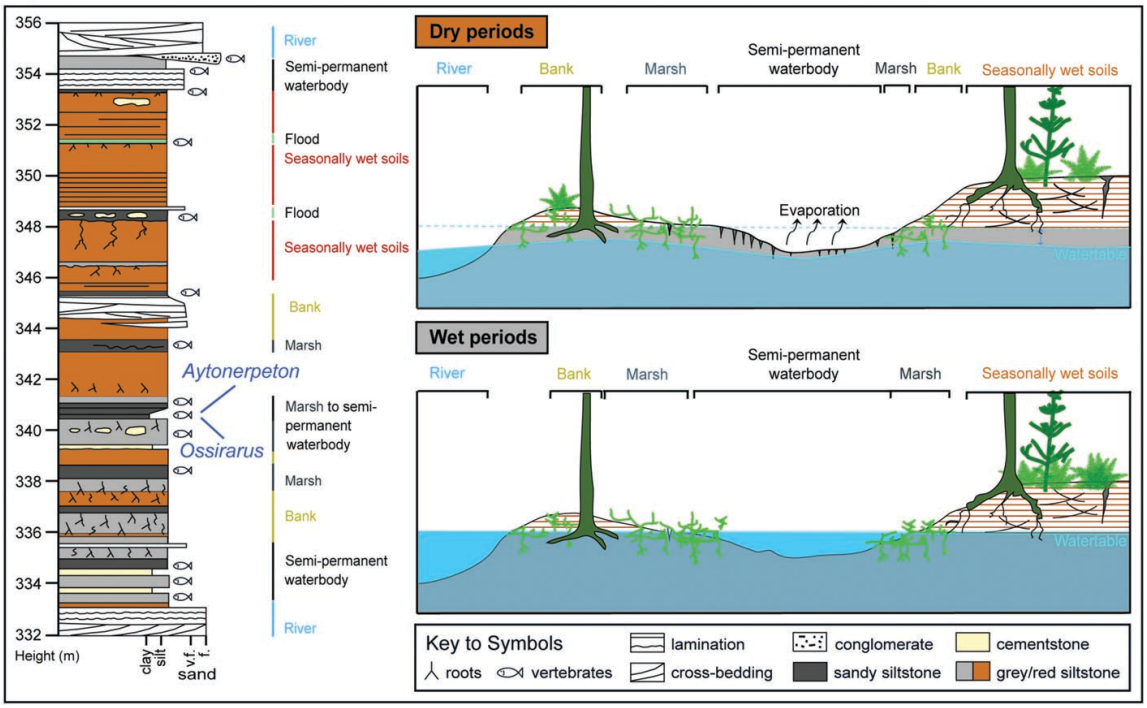

Supplementary Figure 8: Three cladograms. **a**, Majority rule consensus of 4718 trees, unweighted analysis; **b**, Strict consensus of 4 trees, implied weights analysis with k=5; **c**, Strict consensus of 4 trees, implied weights analysis with k=10. The majority rule consensus is of identical topology to this, and the simple weighted analysis almost identical.

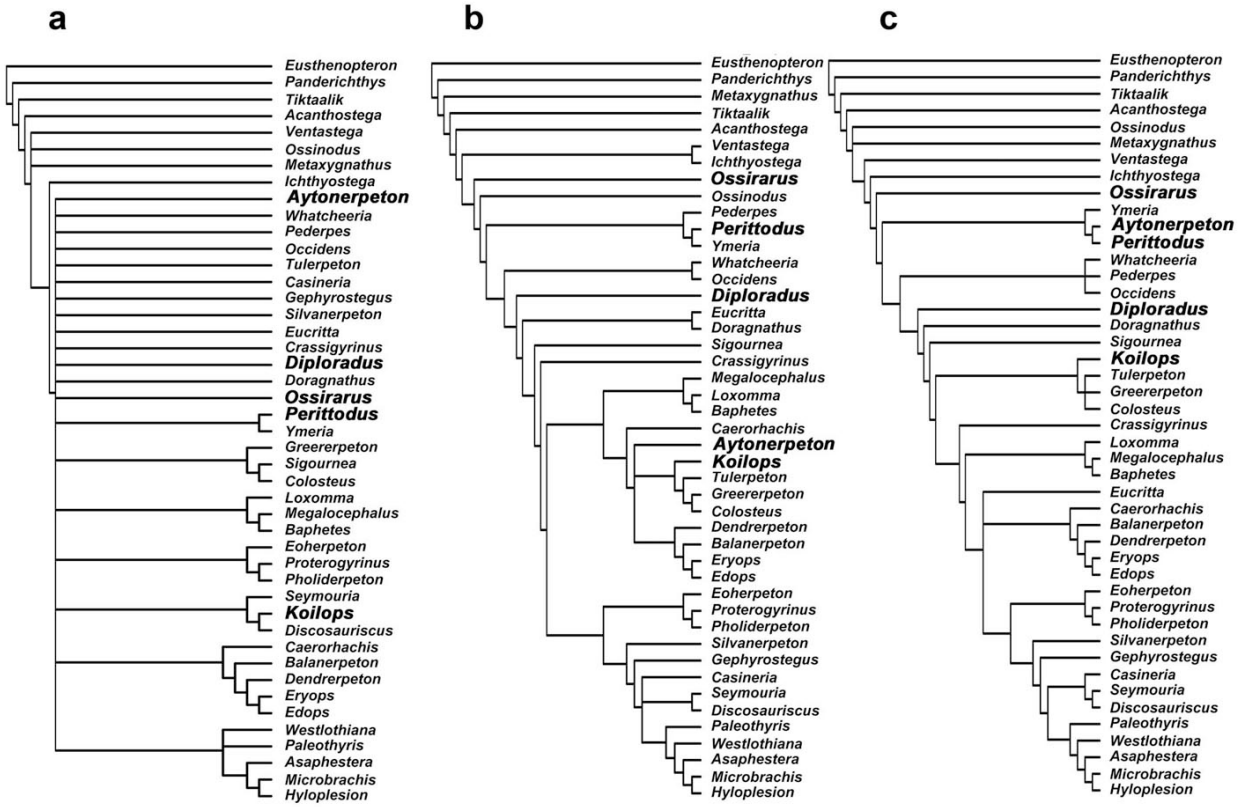

Supplementary Figure 9. Visean fusinite abundance in Euramerica, based on analysis of material from the Stensiö Bjerg Formation (Greenland), Burnmouth Shore/Willie's Hole, and the Strathclyde Group (Fife, Scotland). White bars indicate mean values.

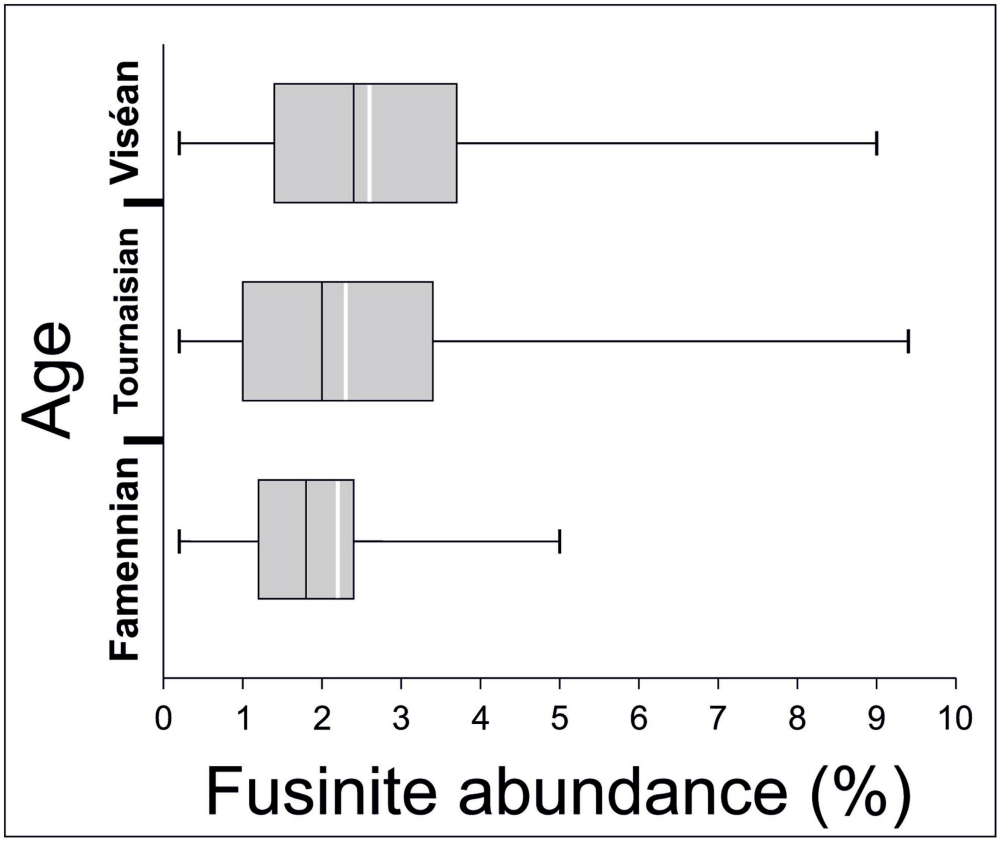

Character List

Unless otherwise stated, characters drawn from publications below, with their numbers

***Ahlberg & Clack 1998[74]; Δ Clack 1998[75]; $Ruta et al. 2002[29]; #Clack & Finney 2004[14]; %Ruta & Clack, 2006[30]; @Klembara et al., 2014[31]; ◊Clack et al. 2012[44]**

Skull roof and braincase

1. Anterior tectal (accessory dermal bone associated with naris having surface ornament and absent lateral line canal; treated here as septomaxilla): present = 0, absent = 1 **$8; #1**
2. Anterior tectal: narial opening ventral to it = 0: narial opening anterior to it = 1 **#2**
3. Basioccipital: indistinguishable from exoccipitals = 0, separated by suture = 1 **#3; %242**
4. Basioccipital: ventrally exposed portion longer than wide = 0, shorter than wide = 1 **#4; %243**
5. Basioccipital: condyle: absent, notochordal = 0 present = 1 **$165; #5**
6. Basipterygoid junction: basipterygoid process fits into socket recessed into epipterygoid = 0, pterygoid/epipterygoid forms narrow bar and clasps basipterygoid process fore and aft = 1 **#6**
7. Exoccipitals: meet skull table: absent = 0, present =1 **#7**
8. Exoccipital contributes to condyle: absent = 0, present = 1 **#8**
9. Exoccipitals enlarged to form double horizontally orientated occipital condyle, (may exclude basioccipital from articular surface): absent = 0, present = 1 similar to **$161; #9**
10. Frontal – parietal length ratio: frontals shorter = 0; longer = 1, subequal = 2 similar to **$35; #10**
11. Frontal anterior margin wedged between nasals: absent = 0, present = 1 similar to **$38; #11**
12. Frontal – nasal length ratio: frontals approximately equal to or less than one-third as long as nasals = 0, more than one-third as long = 1 similar to **$13; #12**
13. Intertemporal present: present = 0, absent = 1 **$60; #13**

14. Intertemporal smaller than supratemporal = 0, or larger than/comparable in size with supratemporal = 1 **modified from %45**
15. Intertemporal lateral edge: not interdigitating with cheek = 0, interdigitates = 1 **$61; #14**
16. Intertemporal contacts squamosal: absent = 0, present = 1 **$62; #15**
17. Jugal deep below orbit (vs narrow process): 50% - > 50% orbit diam = 0, <50% = 1 **$91; #16**
18. Jugal contribution to orbit margin: less than one-third = 0, equal to or more than one-third = 1 Δ**7**
19. Jugal alary process on palate: absent = 0, present = 1 **$90; #17**
20. Jugal length of postorbital region relative to one-third of the length of the postorbital cheek region: greater = 0 or less =1 **not previously used**
21. Jugal extends anterior to anterior orbit margin: absent = 0, present = 1 $**94; #18**
22. Jugal not interposed between maxilla and quadratojugal thus not contributing to skull lower margin = 0 or interposed = 1 = **#21; @27**
23. Jugal V-shaped indentation of posterodorsal margin: absent = 0, present = 1 **$93**
24. Lacrimal contributes to narial margin: absent, excluded by anterior tectal = 0: present = 1, absent, excluded by nasal/maxillary or prefrontal/maxillary suture = 2 **#19; %244**
25. Lacrimal reaches orbit margin (= prefrontal/ jugal suture): present = 0, absent = 1 =$24; #20
26. Maxilla sutures to vomer: absent = 0, present = 1 **$121; #22**
27. Maxilla external contact with premaxilla: narrow contact point not interdigitated = 0, interdigitating suture = 1 **#23; %245**
28. Maxilla highest point in posterior half = 0, anterior third of its length = 1, or at its midlength = 2 **@44**
29. Maxilla extends behind level of posterior margin of orbit: present = 0, absent = 1 modified from **$98; #24**
30. Maxilla sutures to prefrontal: absent = 0, present = 1 **$21**
31. Maxilla – premaxilla contact shelf-like mesial to tooth row on palate: absent = 0, present = 1 **$7; #31**

32. Median rostral (=internasal): mosaic = 0, paired = 1, single = 2, absent = 3 **#25**
33. Nasals contribute to narial margin: absent = 0, present = 1 **#26; 247**
34. Nasal – parietal length ratio less than 1.45 = 0 or greater than 1.45 = 1 **=$15; #27**
35. Nasal smaller in area than postparietal: absent = 0, present = 1 **#28**
36. Opisthotic paroccipital process ossified and contacts tabular below post-temporal fossa: absent = 0, present = 1, post-temporal fenestra absent = 2 **#29; in part %81**
37. Opisthotic forms substantial plate (with supraoccipital if present) beneath skull table, separating it from the exoccipitals: present = 0, absent = 1 **$168; #30**
38. Parietal meets tabular: absent = 0, present = 1 **$39; #31**
39. Parietal – postorbital suture: absent = 0, present = 1 **$40; #32**
40. Parietal anterior portion extent relative to orbit midlength: in front of = 0, level with = 1, posterior to = 2 **$41; #33**
41. Parietal shape of anteriormost third: not wider than frontals = 0, at least marginally wider = 1 **$42; #34**
42. Parietal – postparietal suture strongly interdigitated: absent = 0, present = 1 **$45; #36**
43. Postfrontal – prefrontal contact: broad = 0; or point-like = 1 **@10**
44. Postfrontal – prefrontal suture: anterior half of orbit = 0, middle or posterior half of orbit = 1, absent = 2 **#43; @9**
45. Postorbital suture to skull table (intertemporal or supratemporal) interdigitating vs smooth: smooth = 0, interdigitating = 1 **#37**
46. Postorbital without distinct dorsomedial ramus for postfrontal = 0, with incipient ramus = 1, with elongate ramus = 2. **@14**
47. Postorbital shape: irregularly polygonal = 0, broadly cresentic and narrowing to a posterior point = 1 **$78; #38**
48. Postorbital longer than anteroposterior width of orbit: absent = 0, present = 1 **not previously used**
49. Postorbital at least one quarter of the width of the skull table at the same transverse level: absent = 0, present = 1 $81; **#40**
50. Postparietal: longer than wide = 0, approximately square or pentagonal = 1, wider than long = 2 similar to $49 but split; **#41**

51. Postparietal occipital flange exposure: absent = 0, present = 1 reworded from $52; **#42**
52. Postparietal – exoccipital suture: absent = 0, present = 1 **$51**
53. Prefrontal less than three times longer than wide: present = 0, more than, = 1 $16; %13
54. Prefrontal enters naris: absent = 0, present = 1 **$20**
55. Prefrontal contributes to half or more than half anteromesial orbit margin = 0, less than half = 1 **$22**
56. Premaxilla posterodorsal alary process onto snout: absent = 0, present = 1 $1; #44
57. Premaxilla forms part of choanal margin: broadly = 0, point = 1, not, excluded by vomer = 2 #**45; %251**
58. Preopercular present = 0, absent = 1 **$99; #46**
59. Squamosal posterodorsal margin shape: convex = 0, sigmoid or approximately straight = 1, entirely concave = 2 **similar to $84 but split; #47**
60. Squamosal contact with tabular: smooth = 0, interdigitating = 1, absent = 2 **similar to $71 but split; #48**
61. Squamosal suture with supratemporal position: within skull table = 0, at apex of temporal embayment = 1, dorsal to apex = 2, ventral to apex = 3 **#49; %252**
62. Squamosal anterior part lying behind mid-parietal length: present = 0, absent = 1 **$83; #50**
63. Squamosal interdigitating suture with supratemporal: absent = 0, present = 1 **$66; #53**
64. Squamosal contacts tabular on dorsal surface: absent = 0, present = 1 **$70, %53**
65. Supratemporal present as a separate ossification: present = 0, absent = 1 **$63; #51**
66. Supratemporal forms part of skull margin posteriorly: absent = 0, present = 1 **#52**
67. Tabular lateral horn (subdermal unornamented component): absent = 0, button = 1, blade = 2 **similar to $68+69; #54**
68. Tabular prolonged posterolateral ornamented surface absent = 0, present = 1; **@17**
69. Tabular emarginated lateral margin: absent = 0, present = 1 **#55; %253**

70. Tabular occipital flange exposure: absent = 0, extends as far ventrally as does postparietal = 1, extends further ventrally than does postparietal = 2 **similar to £74 but split; #57**

Palate

71. Ectopterygoid as long or longer than palatines: present = 0, absent = 1 **$137; #58**
72. Ectopterygoid reaches subtemporal fossa: absent = 0, present = 1 **#59; %256** (corrected: subtemporal fossa, not adductor fossa)
73. Ectopterygoid – palatine exposure: more or less confined to tooth row = 0, broad mesial exposure additional to tooth row = 1 **#60; %257**
74. Lateral rostral present: present = 0, absent = 1 **$9 %6**
75. Parasphenoid grooved ventrally about half of length = 0, vs narrow V-shaped section cultriform process along whole length = 1, flat and more or less broad = 2 **#65**
76. Parasphenoid cultriform process shape: biconvex = 0, narrowly triangular =1, parallel-sided = 2, or with proximal constriction followed by swelling = 3 **modified from Δ47**
77. Parasphenoid depression in body: absent = 0, single median = 1, double = 2 **$171+172; #66**
78. Parasphenoid posterolateral wings (ridged): absent = 0, present = 1 **$170; #67**
79. Parasphenoid wings: separate = 0, joined by web of bone = 1 **#68; 260**
80. Parasphenoid contacts or sutures to vomers: present = 0, absent = 1 **#69; 261**
81. Parasphenoid carotid grooves: curve round basipterygoid process = 0, lie posteromedial to basipterygoid process (or enter via foramina there) = 1, absent = 2 **#70; 262**
82. Parasphenoid/basisphenoid ventral cranial fissure: not sutured = 0, sutured but traceable = 1, eliminated = 2 $**9; #71**
83. Pterygoids separate in midline = 0, meet in midline anterior to cultriform process = 1 **$145; #61**
84. Pterygoids flank parasphenoid for most of length of cultriform process = 0, not so = 1 **#62**

85. Pterygoid quadrate ramus margin in adductor fossa: concave = 0, with some convex component = 1 **=$143; #63**
86. Pterygoids not visible in lateral aspect below ventral margin of jugal and quadratojugal = 0, or visible = 1 **#64; @50**
87. Pterygoid junction with squamosal along cheek margin: unsutured = 0, half and half = 1, sutured entirely = 2 **#64**
88. Vomers separated by parasphenoid > half length: present = 0, absent = 1 **#72**
89. Vomers separated by pterygoids: for > half length = 0, < half length = 1, not separated = 2 **#73**
90. Vomer contributes to interpterygoid vacuity: absent = 0, present = 1 $120; **#87**
91. Vomers as broad as long or broader = 0, about twice as long as broad or longer = 1 **modified from $117; #74**

<u>Upper Dentition</u>

92. Ectopterygoid fang pairs: present = 0, absent = 1 **#76; ◊30**
93. Ectopterygoid row (3+) of smaller teeth: present = 0, absent = 1 **$138; #77**
94. Ectopterygoid denticle row lateral to tooth row: present = 0, absent = 1 **modified from #78**
95. Ectopterygoid / palatine shagreen field: absent = 0, present = 1 **$136; #79**
96. Maxilla tooth number: > 40 = 0, 30-40 = 1, < 30 = 2 **#80; ◊33**
97. Maxillary caniniform teeth (about twice the size of neighbouring teeth): absent = 0, present = 1 **#81**
98. Palatine fang pairs: present = 0, absent = 1 **$127; #82**
99. Palatine row of smaller teeth: present = 0, absent = 1 **$130; #83**
100. Palatine denticle row lateral to tooth row: present = 0, absent = 1 modified from #84
101. Parasphenoid shagreen field: present = 0, absent = 1 **#85; %270**
102. Parasphenoid shagreen field anterior and posterior to basal articulation = 0, posterior to basal articulation only = 1, anterior to basal articulation only = 2 **#86; %271**

103. Pterygoid shagreen: dense = 0, a few discontinuous patches or absent = 1 **#87; %272**

104. Premaxillary teeth with conspicuous peak: absent = 0, present = 1 **#89; %274**

105. Premaxillary tooth number: > 15 = 0, 10 - 14 = 1, < 10 = 2 **#90**

106. Vomer fang pairs: present = 0, absent = 1 **$118; #91**

107. Vomerine fang pairs noticeably smaller than other palatal fang pairs: absent = 0, present = 1 **#92; ◊38**

108. Vomer anterior wall forming posterior margin of palatal fossa bears tooth row meeting in midline: present = 0, absent = 1 **=$122; #93**

109. Vomerine row of small teeth : present = 0, absent = 1 #74; **modified from @60**

110. Vomerine shagreen field: absent = 0, present = 1 **$119; #95**

111. Vomerine denticle row lateral to tooth row: present = 0, absent = 1 **#96; %279**

112. Vomer with toothed anterolateral crest: present = 0, absent = 1 **$122; %89**

113. Upper marginal teeth number: greater than lower = 0, same = 1, smaller than lower = 2 **=$221 but split; #97**

<u>Lower jaw characters</u>

114. Adductor fossa faces dorsally = 0, mesially = 1 **$217; #98**

115. Angular mesial lamina interdigitating suture with prearticular: absent = 0, present = 1 $195; #99

116. Angular reaches posteriormost point of lower jaw: absent = 0, present = 1 **$197; #100**

117. Coronoid (anterior) contacts splenial: absent = 0, present = 1 **$189; #101**

118. Coronoid (anterior) contacts postsplenial: absent = 0, present = 1 **#102**

119. Coronoid (middle) contacts postsplenial: absent = 0, present = 1 **◊47**

120. Coronoid (middle) separated from splenial: present, by prearticular = 0, absent = 1, present, by postsplenial = 2 **@98 (in part); ◊46**

121. Coronoid (posterior) posterodorsal process: absent = 0, present = 1 **$214; #103**

122. Coronoid (posterior) posterodorsal process visible in lateral view: absent = 0, present = 1 **$215; #104**

123. Coronoid: at least one has fang pair recognisable because at least twice the height of coronoid teeth: present = 0, absent = 1 $**203+204+211/+213; #105**

124. Coronoid: at least one has fangs recognisable because noticeably mesial to vertical lamina of bone and to all other teeth: present = 0, absent = 1 ◊**11**

125. Coronoid: at least one has organised tooth row: present = 0, absent =1 **modified from $205**

126. Coronoid: at least one carries shagreen: absent = 0, present = 1 **modfied from $204; #106**

127. Coronoid with a row of very small teeth or denticles lateral to tooth row: present = 0, absent = 1 **not previously used**

128. Coronoid: size of teeth (excluding fangs) on anterior and middle coronoids relative to dentary tooth size: about the same = 0, half height or less = 1 ◊**77**

129. Dentary with parasymphysial fangs internal to marginal tooth row: present = 0, absent = 1 **#107**

130. Dentary tooth number: more than 70 = 0, 56-70 = 1, 46-55 = 2, 36-45 = 3, less than 35 = 4 **not previously used**

131. Dentary with a row of very small teeth or denticles lateral to tooth row: present = 0, absent = 1 ◊**81**

132. Dentary external to angular + surangular, with chamfered ventral edge and absent interdigitations: absent = 0, present = 1 **$184; #107**

133. Dentary ventral edge: smooth continuous line = 0, abruptly tapering or 'stepped' margin = 1 ***17**

134. Mandibular sensory canal: present = 0, absent = 1 ***46; #109**

135. Mandibular canal exposure: entirely enclosed apart from pores = 0, mostly enclosed = 1, mostly or entirely open = 2 **$116; #110**

136. Mandibular oral sulcus/ surangular pit line: present = 0, absent = 1 **#111; =◊48**

137. Meckelian bone visible between prearticular and infradentary series: present = 0, absent = 1 **#112; %282**

138. Meckelian bone or space exposure in middle part of jaw, depth much less than prearticular = 0, depth similar to prearticular = 1 ◊**26**

139. Meckelian foramina/ fenestrae, dorsal margins formed by; Meckelian bone = 0, prearticular = 1, infradentary (postsplenial) = 2 ◊**25**

140. Adsymphysial tooth plate: present = 0, absent = 1 **%178; #113**

141. Adsymphysial plate fang-pair (distinct from other teeth): absent = 0, present = 1 **$179; #114**

142. Adsymphysial plate dentition: shagreen, denticles or irregular tooth field = 0, organised dentition aligned parallel to jaw margin = 1, no dentition = 2 **$180+181; modified from ◊30**

143. Adsymphysial lateral foramen present: absent = 0, present = 1 ◊**28**

144. Adsymphysial mesial foramen present: absent = 0, present = 1 ◊**29**

145. Postsplenial with mesial lamina: absent = 0, present = 1 **$192; #115**

146. Postsplenial pit line present: present = 0, absent = 1 **$193; ◊48**

147. Postsplenial suture with prearticular: absent = 0, present but interrupted by Meckelian foramina or fenestrae = 1, uninterrupted suture = 2 ◊**35**

148. Prearticular shagreen field, distribution: gradually decreasing from dorsal to ventral = 0, well defined dorsal longitudinal band = 1, scattered patches or absent = 2 ◊**42**

149. Prearticular sutures with surangular: absent = 0, present = 1 ◊**39**

150. Prearticular with longitudinal ridge below coronoids: absent = 0, present = 1 ◊**37**

151. Prearticular centre of radiation of striations: level with posterior end of posterior coronoid = 0, level with middle of adductor fossa = 1, level with posterior end of adductor fossa = 2 ◊**36**

152. Splenial, rearmost extension of mesial lamina closer to anterior margin of adductor fossa than to the anterior end of the jaw: absent = 0, present = 1 **$188; #116**

153. Surangular crest: absent = 0, present = 1 **#117; ◊44**

<u>General skull characters</u>

154. Skull longer than broad = 0, as broad as long =1, or broader than long = 2 **@3**

155. Preorbital region of skull less than twice as wide as long = 0, or at least twice as wide as long = 1 **@4**

156. Anterior palatal fenestra: single = 0, double = 1, absent = 2 **$159; #118**

157. Internarial/ interpremaxillary fenestra (independent of presence of median rostrals): absent = 0, present = 1 **$102; #119**

158. Interorbital distance compared with maximum orbit diameter: greater = 0, smaller = 1, subequal = 2 **$120**

159. Interpterygoid vacuities: absent = 0, at least 2 x longer than wide = 1, < 2 x longer than wide = 2 **$154+156; #122**

160. Naris position: ventral rim closer to jaw margin than height of naris = 0, distance to jaw margin similar to or greater than height of naris = 1 **#123; %283**

161. Naris shape: slit-like = 0, round or oval = 1, upper margin ragged = 2 **#124; %284**

162. Naris shape: ventrally facing = 0, dorsolaterally facing = 1 **#125; %285**

163. Orbit shape: round or oval = 0, angle at anteroventral corner = 1, angle at posteroventral corner = 2: emarginated margin including jugal, lacrimal and prefrontal = 3 **modified from $105; #127**

164. Orbit position re snout/postparietal length: centre closer to front than rear = 0, centre near middle = 1, centre closer to rear than front = 2 #128; **@1**

165. Orbit position re snout /quadrate length: centre closer to front than rear = 0, centre near middle = 1, centre closer to rear than front = 2 **#129**

166. Pineal foramen position along interparietal suture: behind midpoint = 0, at the midpoint = 1, anterior to midpoint = 2 **$107; #130**

167. Suspensorium proportions: quadrate to anterior margin of temporal embayment about equal to maximum orbit width (discounting any anterior extensions) = 0, quadrate to anterior margin of temporal embayment < maximum orbit width = 1, quadrate to anterior margin of temporal embayment > maximum orbit width = 2 **#132; %287**

168. Skull table/cheek junction: smooth profile = 0, square/ abrupt profile = 1 #133

169. Skull table shape: longer than broad = 0, approximately square = 1, shorter than broad = 2 **#134; @**3

170. Ornament character: regular, dense, but no star-burst pattern = 0, fairly regular pit and ridge with star-burst pattern at regions of growth = 1, irregular but deep = 2, irregular but shallow = 3, absent or almost absent = 4 **#135; %288**

Postcranial characters

171. Centra: intercentrum dominant = 0, pleurocentrum dominant = 1, holospondylous = 2 **modified from #136 & %289**

172. Centra strongly notochordal such that notochordal space more than 2/3 diameter of entire centrum: present = 0, absent = 1 **not previously used**

173. Centra (trunk) pleurocentra fused midventrally: absent = 0, present = 1 **$293; #137**

174. Centra (trunk) pleurocentra fused middorsally: absent = 0, present = 1 $295; **#138**

175. Centrum (sacral) not distinguishable by size or shape from pre- and postsacrals = 0, distinguishable = 1 **#139; %290**

176. Clavicles meet anteriorly: present = 0, absent = 1 **$228; #140**

177. Cleithrum co-ossified with scapulocoracoid = 0, separate = 1 **$227; #42**

178. Cleithrum smoothly broadening to spatulate dorsal end = 0, distal expansion marked from narrow stem by notch or process or decrease in thickness = 1, end simply tapering = 2 **#142; %291**

179. Cleithrum stem cross section at mid section, flattened oval = 0, complex = 1, single concave face = 2 **#143; %292**

180. Humerus ends more or less untorted = 0, ends offset by > 60 degrees = 1 #**152; %294**

181. Humerus L-shaped = 0, waisted but no shaft = 1, with distinct and slender shaft = 2 **$247 split; #143**

182. Humerus accessory foramina present = 0, absent = 1 **$254; #154**

183. Humerus latissimus dorsi process part of ridge = 0, distinct but low process = 1, spike = 2 **#155; %295**

184. Humerus latissimus dorsi process position compared with deltopectoral crest: more proximal to head = 0, equidistant from head = 1 **#156**

185. Humerus latissimus dorsi process position relative to ectepicondyle: offset anteriorly = 0, in line = 1 **$238; #157**

186. Humerus latissimus dorsi process confluent with deltopectoral crest: present = 0, distinct from = 1 **$241; #158**

187. Humerus anterior margin: smooth finished bone convex margin = 0, anterior keel with finished margin = 1, cartilage-finished = 2, smooth concave margin = 3 **#159**

188. Humerus radial facet position: distal and terminal = 0, anteroventral = 1, ventral = 2 **$248 split; #160**

189. Humerus radial/ulnar facets: confluent = 0, separated by perichondral strip of bone = 1 **similar to $239; #162**

190. Humerus with distinct supinator process: absent = 0, present = 1 **$240; #163**

191. Humerus with ventral humeral ridge: present = 0, absent = 1 **$244; #164**

192. Humerus ectepicondyle distinct: present = 0, absent = 1 **$246; #165**

193. Humerus ectepicondylar ridge distal end aligned with ulnar condyle = 0, between radial and ulnar condyles = 1, aligned with radial condyle = 2 **$246; #165**

194. Humerus entepicondyle width relative to half humeral length: greater = 0, less = 1 **$252; #166**

195. Humerus entepicondyle width relative to humeral head width: smaller = 0, greater = 1 **$253; #167**

196. Interclavicle body shape (distinguished from parasternal process): rhomboid, longer than broad = 0, broader than long = 1 $**231+232; #169**

197. Interclavicle parasternal process shape: absent or tapering = 0, parallel sided = 1 **$230; #170**

198. Neural arch ossification: paired in adult = 0, single in adult = 1 **#171; %298**

199. Neural arch (atlas) halves fused: absent = 0, present = 1 **#172**

200. Neural arches with distinct convex lateral surfaces ('swollen'): absent = 0, present = 1 **#174; %220**

201. Neural arches of trunk vertebrae fused to centra: absent = 0, present = 1 $**296; #175**

202. Radius: longer than ulna = 0, same length as ulna = 1, shorter than ulna (including olecranon process if present) = 2 #1**78; %186**

203. Ribs (trunk): straight = 0, ventrally curved = 1 **$280; #179**

204. Ribs (trunk) not longer than height of neural arch plus centrum = 0, less than 2.5 x height of neural arch plus centrum = 1, more than 2.5 x height of neural arch plus centrum = 2 **#180; %302**

205. Ribs (trunk) tapered distally or parallel-sided = 0, expanded distally into overlapping posterior flanges = 1 modified from **$282; #181**

206. Ribs (trunk) bear proximodorsal (uncinate) processes: absent = 0, present = 1 modified from **$281; #182**

207. Ribs (trunk) differ strongly in length and morphology along 'thoracic' region: absent = 0, present = 1 **#183; %305**

208. Ribs (cervical): flared distally = 0, tapered distally = 1 **#184**

209. Scapulocoracoid dorsal blade: absent = 0, present = 1 **#187; %308**

210. Scapular ossification separate from coracoid: absent = 0, present = 1 **$233; %188**

211. Gastralia: tapered and elongate, 4 or >4 x longer than broad = 0, ovoid = 1, around 3 x longer than broad one end tapering = 2 **#189; %309**

212. Pelvis: illium, ischium, pubis not separate ossifications = 0, separate = 1 **#176**

213. Illium: post illiac process and dorsal blade present = 0, only post iliac process present = 1 **modified from $259; #165**

```
#NEXUS
begin data;
dimensions ntax=45 nchar=213;
format missing=? symbols="0~4";
matrix
Acanthostega
0000000001001???000000100001001100000011010000001000000010000000000100010100001
211000011?01000000000200100000001000100000?1100010111001110101001010101000001120
0000110001000001000001000000110001000 1?00000000000000
Asaphestera
1?1?101112001???11?001010111100310 0?1102011110000011000021 11?0?11000011?11??????
??001?01200???1?0?????002???????1??1?????????????????011?1????????1???????11?0020
110221?1232111??1??121????3??????1?101?01?12000?10?10
Balanerpeton
1?11?1?101?100101001000100?20003100??002011111 10020?0011112221100100100111200?0
2201102121001111001101101001111101111112??11111?141001?11?210?001122?0?00?12012?
11000210210?00?112??11????3???1??1?00100010100001?111
Baphetes
01???00??1100010?100?100?0010001110100020 10?110?010000?0110231100110000111112 0?1
0210012120101111001110001001111 1?????????????????????????????????????????0020000
0132102011?0????121001210120001021?????????????????010
Diploradus
?????0?10????????1??000???0100?????????????1?????????????0??0?????????????????10?1?
?21000?????????1????0?002???????10001000??110011121??00?101002??0?0200000?????0?
??????2??24?????????????????????????????????????????
Ossirarus
??1????10???01??00?0000?????0????????1???0?0100001?????????2???0000100?????????
??????????????????????????????????????????????????????????????????????????????
??0????1041000??111001????010000???000?00??????????2??
Caerorhachis
?????0??????00?000???00??1?1000?1????0021101111?02??0??011??111?0?0?10001??210??
?21100?1100011100011010 0?01111111 1?1000101111?011??1??101010001?10?0?10002002?
?1?111??211010?????????????????????????1?00?110000??010
Casineria
??????????????????????????????????????????????????????????????????????????????
??????????????????????????????????????????????????????????????????????????????
??????????1?1???12?111????32??10?1???1?0021200111121?
Colosteus
1????0???1111???11?00?0201010103011 0?0121100100111??111011000011000000 1?1112???1
?21100?1100001010011??0011?100110110????0???0?1?0411002?111?????0???1???00010010
110000200 1?000?01?????????????????001?001???1????0??
Crassigyrinus
1??1?00??200000000?0000101110013100??0021111000001000100211211000111 1?0001111101
22?0001100000101000102000000101010 1?0000??11111?1410102110100100010210110001110 1
2111002102?01??11?1000111120001 0?110000001120 00???010
Dendrerpeton
1????1???0000010110010010111000310 0??0021100101002??0001?122201001001???11120 0?0
12011021211???0001101001011111101101??1?????????3101 1?110?????112210??10021011
110111012100 00?111?111????32?010?1?00??00211000010111
Doragnathus
??????????????????????????????????????????????????????????????????????????????
??????????????????????????????010????0011001110101 1?11011??001112?0?101??????
??????????????????????????????????????????????????11
Discosauriscus
0111?0010201011111010101000110031 01??102111110100210000001222110011002011 12?0111
```

??011111001111020011020020011011211110001111111113100 1?11?11??00112200?111120210
1100121123111101 2?0011001300010?1?111110211001011110
Edops
0111111101000010000010001011000300011002010010111211000?11?2?1100?1011011111200?1
02111?212000111200110?002011111211?1???1?11111?0310?1?1??????0011??10???0020011
0102202021 0?00????111????32?111?11??????????????1??
Eoherpeton
?????????10000011?010011?0100?3100??10211?10000021?0000?1121?0000100?0?01??111?
221?1??????101020011??002?????????????????110111???0?1?1101????1112?0??100?10?0
110112112211 10??1??0010011010110201??1?00?1200??1??10
Eryops
0?111111110 01???000110001011000311011001010010000211001111221110000101011123 00??
0201102121001111101 11?0110111111111110211111 11?021011?11?1???00112210?010020011
1102202121010011112111110132011020110100020101 1010?11
Eucritta
1????????2000010 10?000010?010003?00??002111010000 2??000??112201001000????1?110?1
121?1??????????110??000??0?????????????????????????0?1?1?????????????????000?01??
??12111?21????110??01?????????????00?????0?00?01?010
Eusthenopteron
0000000000000100000000000000000000110000100000000000000000?100000000000?00?10000
200000002?0010000010020000001000100000000?0000010000000000000000??0?0000?000000001
0?000120000000001?00?0????000000010??0?000000000100?0?
Gephyrostegus
1????0???110010110000102000200031 00??102111100100 21?000001121100011101111111 10?0
221011?120101111100111?0020111111111110111101111?031001?11011????1112?0?110020200
1102121114111011122?01????0????0???1?100021200101?010
Greererpeton
1?0110110111101000000002000101030011101211001001111111101101001100100111111221 00
2211002110000100000101011101101101???1111111?1410102111101100010200?110011010
1101100001000 0?011?0011011000110?0100100020101011 0211
Hyloplesion
1????????0011???100001010001100311 0??112111010000 2??00101101?10110000?11?12100?0
220110?121111112111102002 1?110110?????????????????41001?1?????????1?????11120010
110002?12421111?12??2?????321?11???1011002120001 10?11
Ichthyostega
0010000002001???000000000101001 2000??000010010000 1?000002001001000001?111??100?1
211000011?0101020101 1?1121?100102000100 00?0100110410000110101101000201000000000
0001101011000 0?1000000?????11?000011 10?0021211 1?00000
Loxomma
01???0???2000010??00?000?00?000?100110021 10?111?010000?0110231100110000?111120??
02????????0011020011??0020011011?11?????1????1??????021101?????111?1?1?000?0??0
013220?011???
Metaxygnathus
??
??????????????????????????????????000000000000001?310002010?011?10?0100000??????
?????????3???
Megalocephalus
0?111001010 01?????10?002?0010001110100020 10?100?020000?0110231100110000111112 0?1
0210002120001111001100002001111101101000 0?11101?1410102110201100112210?000000?00
1132202021???
Microbrachis
??111011100 11???1000010?00?110031100111211011001021100100101?0?11?000111?11100?1
120110000011111201110000 21?110111111100010111 11?1410102110 11????112200?110120010
110002?1212111?112??11????3???11???100110212000 11?111
Occidens
??

????????????????????????????????????100???010011??10102??10?????010????????????
?????????2??
Ossinodus
?????0??????1????010000?0?0100????0??0121101 1?00120???0??0121110010 00?0111??????
??1?00?1100101001001???0?1000000???001?200
?1?100011???00
Paleothyris
1?111000010 11???10?1010100011003100?0112111210000210001001 12?0?0010002???1?120?1
?2111101201??0111110210 21?11111???1?????????????????11?1?????????1??????10020110
110112111311111101??121????3201102 1?1100121200001102??
Panderichthys
00000000000?000000?000000002000000??100000100100110000000001210000000000?00??0000
?000??002000000??000?2?0?00000?0?00??0?0??0000000?0000000??000??0?0101??00000000
00?00121000000??10?000000?000000010??0?00000000?00?10
Pederpes
1????0??????01?111??0??10?00000?1????00??100?100021?0010?0123010011002010?03?101
?210???11?10011210010?0?200101 11???1????????0??1????1021??????????0?0???000???00
21221?212100000111100121012??110?0?000000102111011210
Pholiderpeton
0?111001010001100110100210010003110201020110100002100000110?110002111200011111 11
021010011010010010111?0021?110111111100?1111111??310102011100200111211?110020210
210221011211111111?0?????????1011?00100021200001 02??
Proterogyrinus
1?111001010001001100?011??010030000001021110000002100 0?0?112110001211200011311 11
021111?????101000011010 02??????111010 00??0??1??021011?1111??????1???1?1100?0210
110212211311101111?00111112 2?110001001000212000010210
Seymouria
0?111011020001110101010100111003100211021101100002111000012221100100020111111111
221011210011111200111?002001101121111000111111??41001?11?11??00112200?110020000
111112012111111011111111?1321111?101111112111010 11?10
Sigournea
??
?????????????????????????????????11?10001?110011001?002110?0????010200?10???????
?????????3??
Silvanerpeton
1?1110???200010012?001010??11003100??102?111001001??0010?110110100200???11?110?1
22101??1001???1100110000 2????????11?1??????111111??21001????1???????1?????00020100
110112110310 10?111?001????1????0?1000?000212000010210
Tiktaalik
?????0??????1???00?11???0??????0?????000110000110??1?0??012110001000????????0?0
20000??0?0?????????????????????????00010000?0100?0??100???0000????0?00????000?0200
?012102020??????10?000????0010001 10??????00?100??0?0?
Tulerpeton
????????????????1?1?101?????????????????02?100?????????????01??????001010?????????
??????????0?????????????110?10111??1?????????????????????02????????????????????????
?????2???100???0111101101100111010100????21?????10010
Ventastega
?????????000?1000100001 1?0100?11?000?110100100 00?000010?012?0?0??0010??1?02????
0?1000?1?00????0000110011000001020001000000000110011000010100111000101000 00?1200
??121?2101????0000?????????????????00????????????0????
Westlothiana
?????0???1011???10??0???0?01?0?3100??112111010100??????0?102?10000000????1??10?1
?21000?1?0????120???1?001???????1??1?????????????210?1?1?????????????????100?0000
110111112411 11??1??121????32?11121???1?0121200011 0?11
Whatcheeria
?????00??110001111?110011?0100?311010001010010000110000 0?0121110011012???????10?

?21????????001011001??0120??000?1000100000110011031?101110001100010101?10???0100
2122200?2400101011??0121012 0?0?0101111?002??11??11?10
Koilops
?????????201????10?10??1?????1?3??????0111101??00???0000?????1????????0??????1??
??????????0???????0?????20??0???012?2??
11011????1???
Ymeria
?????????????????????????????1???00?0??????
??100????0?001?21001???0200100111?00?000000100100411001110101 1?1010101000???????
???
Perittodus
????????????????11?{01}??0???01??0?????????????????????????????????1?????????????????
?????????????????20?????????????????????010?10001001014100??????111??0????1??0????
???????????3?????????????????????????????????1????????0??
Aytonerpeton
?????????????????????00?10001000?1???
?????0?????????200?1??0120111?1?0???1001??111010141000 10??100??????0?????01????0
11???????2?????????????????????????????????????0?0??????11
;
end;

begin trees;
tree tnt_1 = [&R]
(18,(30,(24,(37,(1,((28,(6,(((5,(10,(12,((23,((17,((19,(36,((29,(40,(2,(21,26)))
),(8,(13,34))))),(15,(32,33)))),(7,((14,(11,(3,16))),((42,(38,(9,20))),(35,45)))
))),(4,25))))),(27,41)),(31,(43,44))))),(22,39)))))));

end;

Supplementary Table 1. Table 1a shows the localities, stratigraphy, age, spore zone, environment and number of samples from each site. Table 1b shows the fusinite abundances as a percentage of total phytoclasts taken for each stage sampled.

Extended data table 1a

Locality/references	Stratigraphy	Age	Spore Biozone(s)	Environment	Number of samples
1[76,77]	Pathead Fm	Late Viséan	VF	Deltaic – nearshore marine	8
1[76,77]	Sandy Craig Fm	Mid-Viséan	NM – VF	Fluvio-deltaic	3
1[76,77]	Pittenweem Fm	Mid-Viséan	NM	Deltaic – nearshore marine	14
1[76,77]	Anstruther Fm	Early – mid-Viséan	TC	Deltaic – nearshore marine[2]	13
2[77,78]	Fife Ness Fm	Earliest Viséan	Pu – TS	Fluvio-deltaic	4
3[15,78]	Ballagan Fm	Tournaisian	CM	Fluvio-lacustrine	12
4[15,78]	Ballagan Fm	Tournaisian	VI – CM	Fluvio-lacustrine	61
5[79,80]	Stensiö Bjerg Fm	Latest Famennian	LL – LN[5]	Fluvio-lacustrine	9

Localities: 1, Anstruther to St Monans coastal sections, East Fife, Scotland; 2, Fife Ness, Scotland; 3, 'Willie's Hole', Chirnside; 4, Burnmouth Shore; 5, Celsius Bjerg, East Greenland.

Extended data table 1b

Famennian	**Tournaisian**		**Viséan**
2.4	**Burnmouth**	**Willie's Hole**	4.8
1.8	5.2	2.8	0.8
1.2	4.0	2.4	1.2
0.2	0.6	3.0	6.0
4.2	4.8	3.0	1.8
2.4	1.4	0.6	1.2
1.6	1.6	1.6	2.8
0.8	5.2	2.4	1.0
5.0	4.6	0.6	1.4
	3.0	2.3	2.0
	2.8	3.6	0.4
	0.2	1.2	2.4
	3.4	0.2	2.4
	0.2		1.6
	0.2		2.2
	1.0		2.4
	3.4		4.2
	1.2		0.4
	2.2		2.6
	1.0		2.6

	2.8		3.8
	0.6		9.0
	2.0		2.6
	2.0		0.6
	2.0		1.6
	2.2		1.4
	4.2		2.6
	5.2		0.2
	1.2		0.8
	2.2		3.0
	1.2		4.2
	1.8		2.4
	2.2		2.6
	1.8		0.4
	0.4		3.8
	0.8		3.4
	0.4		3.2
	4.2		5.4
	5.8		4.2
	4.6		2.2
	1.0		4.8
	0.4		4.2
	0.4		
	1.0		
	1.2		
	0.6		
	1.8		
	9.4		
	3.8		
	0.4		
	2.0		
	2.0		
	1.6		
	3.4		
	2.2		
	3.4		
	5.6		
	1.8		
	0.6		
	0.6		
	2.2		
	1.4		

Famennian – Viséan Fusinite abundance (% total phytoclasts)